

**SATELLITE-ESTIMATED CLOUDINESS  
FROM NOAA AVHRR DATA IN THE  
NORDIC AREA DURING 1993**

Karl-Göran Karlsson



SATELLITE-ESTIMATED CLOUDINESS  
FROM NOAA AVHRR DATA IN THE  
NORDIC AREA DURING 1993

Karl-Göran Karlsson



Issuing Agency SMHI S-601 76 NORRKÖPING Sweden	Report number RMK 66	
	Report date June 1994	
Author (s) Karl-Göran Karlsson		
Title (and Subtitle) Satellite-estimated cloudiness from NOAA-AVHRR data in the Nordic area during 1993.		
Abstract <p>A method to estimate monthly cloud conditions (total fractional cloud cover) from multi-spectral satellite data is described. The operational cloud classification scheme SCANDIA (the <u>SMHI</u> <u>C</u>loud <u>A</u>nalysis model using <u>D</u>igital <u>A</u>VHRR data), based on high resolution imagery from the polar orbiting NOAA satellites, is used to produce monthly cloud frequencies for all months of 1993. The annual mean is computed and the diurnal variation of cloudiness is investigated for June and December. Cloud analyses are made for an area covering the Nordic countries with a horizontal resolution of four km.</p> <p>Comparisons with existing surface observations show very good agreement, especially in the summer half of the year. some problems are indicated in the winter season when a minor underestimation of cloudiness is noticed. The underestimation is mainly due to the non-separability of low-level water clouds from cloud-free areas at very low sun elevations. Despite these problems, general cloud patterns are well described also in cold winter situations. Improvements of the method are discussed and an enlargement of the analysis area is envisaged.</p> <p>The method is proposed as a valuable tool for local and regional monitoring of the cloud climatology. Comparisons with forecasted cloudiness from atmospheric models are suggested as well as special studies of cloud conditions in the Polar areas.</p>		
Key words Cloud classification, NOAA-AVHRR, Nordic cloud climatology.		
Supplementary notes	Number of pages 64	Language English
ISSN and title 0347-2116 SMHI Reports Meteorology and Climatology		
Report available from: SMHI S-601 76 NORRKÖPING Sweden		



## Table of contents

	<u>Page</u>
1. Introduction	1
2. SCANDIA - the cloud classification model	1
3. Quality of satellite-derived cloudiness	7
3.1 Comparison with surface observations	7
3.2 Results for the total data set	8
3.3 Results for data with low satellite zenith angles	9
3.4 SYNOP overestimation of cloudiness in summer	10
3.5 Results for the winter season	11
3.6 Distribution of absolute errors	13
3.7 Conclusion of the verification study	14
4. Computation of monthly cloud frequencies	14
5. Cloudiness in 1993	15
5.1 Monthly cloud frequencies	17
5.2 Annual mean of cloud frequencies for 1993	29
5.3 Diurnal variation of cloud frequencies in June and in December	31
6. Discussion	34
6.1 Cloud conditions monitored by SCANDIA	34
6.2 Quality of SCANDIA results	35
6.3 Resemblance to true cloud frequencies	35
6.4 Sensitivity to AVHRR sensor noise and degradation	36
6.5 Climate studies of Cirrus clouds and low-level clouds	36
6.6 Future use and improvement of SCANDIA cloud analyses	37
6.7 Proposals of future studies	38
Acknowledgements	39
References	39
Appendix	



## 1. INTRODUCTION

Satellite imagery is today an indispensable tool for the weather forecaster when diagnosing cloud conditions in the operational forecasting process. The main reason is the superior coverage of large areas with high horizontal (especially for polar orbiting satellites) and temporal (especially for geostationary satellites) resolution compared to surface-based cloud observations from synoptical weather stations (SYNOP).

The experienced forecaster can use satellite images in several spectral bands to identify different cloud types and surface types. This fact has encouraged the development of automatic objective cloud classification schemes to enable quantitative cloud observations from satellite imagery. Several multispectral cloud classification methods, based on data from the AVHRR instrument (Advanced Very High Resolution Radiometer - described by Lauritson *et al.*, 1979) on the NOAA polar orbiting satellites, have been proposed. Some examples are described by Coakley and Bretherton (1982), Arking and Childs (1985), Phulphin *et al.* (1983), d'Entremont (1986), Saunders and Kriebel (1988) and Inoue (1987). Some of them have also been introduced as operational schemes (see for example Derrien *et al.*, 1993).

This report describes a method to estimate regional cloud conditions in the Nordic area from NOAA AVHRR data for a whole year (1993). Monthly, seasonal and annual cloudiness have been estimated by using results from an operational objective cloud classification scheme, developed at the Swedish Meteorological and Hydrological Institute (SMHI).

The basic principles of the cloud classification scheme are presented in Section 2. Section 3 discusses the typical quality characteristics of the satellite-derived cloud information as deduced from recent comparisons with SYNOP observations. The method to estimate monthly cloud frequencies is presented in Section 4. Results for all months of 1993 are given in Section 5, together with the annual mean and a comparison of the diurnal variation of cloudiness in June and in December. Finally, the overall performance of the cloud classification model is summarized and discussed in Section 6. The potential use of the derived information for cloud climate monitoring and for other purposes is also discussed here.

## 2. SCANDIA - THE CLOUD CLASSIFICATION MODEL

The idea of an operational cloud analysis scheme, based on digital AVHRR data, was proposed at SMHI in the early 1980s (Liljas, 1981). Several years of spectral signature studies followed where different cloud and surface types were examined. Typical reflectivity, transmissivity and emissivity characteristics were monitored for each cloud and surface type depending on varying solar elevations, airmass changes and different AVHRR sensors (satellites NOAA-9, NOAA-10, NOAA-11). After defining the main principles for an operational cloud classification method (Karlsson, 1989), the final classification scheme, named SCANDIA (the SMHI Cloud Analysis model using

Digital AVHRR data), was implemented in 1988. A brief description of the main characteristics of the cloud classification model is given below. A full description can be found elsewhere (Karlsson and Liljas, 1990).

The classification model makes use of calibrated and geometrically transformed imagery from all five AVHRR channels (given in Table 1) at maximum horizontal resolution (at nadir 1.1 km). AVHRR scenes are classified by using seven image features and they are listed in Table 2. Classifications are made in two predefined areas, covering the northern and southern parts of the Nordic area. Each pixel in a scene is classified into one of 23 cloud and surface types (see Table 3). The main use of each classification feature is summarized in Table 2. Feature four is central for the classifier. This feature is based on AVHRR channel three brightness temperatures related to brightness temperatures in AVHRR channel four. The feature plays a major role in the cloud/no-cloud discrimination, both day and night. The strength of the feature is to enable discrimination of clouds and snow surfaces during day (as demonstrated by Kidder and Wu, 1984) and to map low and mid-level water clouds during night (as discussed by Eyre *et al.* (1984) and by Saunders and Gray (1985)) despite small temperature differences between the surface and the cloud tops.

Table 1. Spectral bands of the AVHRR instrument.

AVHRR channel	Spectral interval ( $\mu\text{m}$ )
1	0.58 - 0.68
2	0.72 - 1.10
3	3.55 - 3.93
4	10.30 - 11.30
5	11.50 - 12.50

SCANDIA is a supervised thresholding model, where typical class domains are defined by hyperboxes in a seven-dimensional feature space. A unique set of thresholds is defined for each of several predefined categories related to existing illumination conditions, weather types and satellites. The season (one of the set "Summer, Spring, Winter, Autumn"), the current sun elevation (determined by one of 12 defined sun elevation intervals) and the satellite (at present NOAA-11 or NOAA-12) are specifying which category and thus which set of thresholds is used to classify the scene in each of the two areas. In total, 96 different categories are necessary to adapt the cloud classification model to the seasonal and daily changes of classification conditions. A more direct dependence on the current weather situation is furthermore applied by using temperature information at the 700 hPa and 500 hPa levels. This information is taken from meteorological objective analyses and is used for threshold tests of feature five (see Table 2). A schematic example of the hierarchic model structure for one specific classification category is given in Figure 1. Here  $A$  denotes albedo,  $T$  denotes brightness temperature and  $TEX$  is a texture feature (feature seven in Table 2). The index refers

Table 2. Classification features used by SCANDIA. Calibrated AVHRR channels are denoted CH1, CH2, CH3, CH4 and CH5. TEX4 means a local (in a 5x5 pixel window) highpass filtering of CH4 followed by a lowpass filtering (in a 11x11 pixel window) to measure the small scale variation of brightness temperatures.

Feature number	Composition	Quantity	Main use for classifier
1	CH1	Albedo*	Daytime separation of clouds and snow from land surfaces. Used tightly together with feature 4.
2	CH1-CH2	Albedo difference	Daytime separation of land surfaces with vegetation from sea surfaces. Used also for snow detection.
3	Land mask	Land or sea indication	Geographic map used for land/sea-separation at night and for low sun elevations.
4	CH3-CH4	Brightness temperature difference	Separates all clouds from land and sea surfaces during daytime. Important at night for fog, Stratus and Cirrus detection.
5	CH4	Brightness temperature	Separates main cloud groups Low, Medium and High clouds by comparing with mean temperatures at 500 hPa and 700 hPa.
6	CH5-CH4	Brightness temperature difference	Separates thin clouds (especially Cirrus clouds) from thick clouds both night and day.
7	TEX4	Temperature variance	Separates clouds with high small scale texture (e.g. Cumulus) from more homogeneous clouds (e.g. Stratus).

\*This is not a true albedo. A more correct description is bi-directional reflectance.

to AVHRR channel. Some of the most important thresholds are shown in the right part of Figure 1. If the thresholds in a step are matched for the analysed pixel, the labelling is changed to the new class. The increasing number of arrows visualizes the separation into an increasing number of classes for each hierarchic step.

Table 3. *Classified cloud types and surface types.*

Open sea without ice	Cumulus congestus over sea
New ice without snow	Small Cumulonimbus
Snowcover (also on ice)	Extensive Cumulonimbus
Winter forest	Altostratus and Altostratus
Land (free from snow)	Nimbostratus
Haze or sub-pixel clouds over land	Thin Cirrus over land
Haze or sub-pixel clouds over sea	Thin Cirrus over sea
Fog and Stratus	Cirrus over low level clouds
Stratocumulus	Cirrus over middle level clouds
Small Cumulus over land	Thick Cirrostratus
Small Cumulus over sea	Sunglints
Cumulus congestus over land	

Thresholds have been defined by using class mean vectors and covariance matrices from a class database with spectral signatures in the seven-dimensional feature space. This database was defined earlier in the signature study phase. The choice of thresholds was defined subjectively but in a consistent manner, guided by the class database information. The use of a simple thresholding model instead of a more sophisticated statistical model (e.g. a maximum-likelihood classifier) was decided for practical reasons. Operational requirements are putting hard constraints on a cloud classification scheme. Furthermore, it was considered more fruitful to put the main effort into creating a realistic structure for the model (e.g. dependence on sun-elevations, seasons etc.) to enable a dynamic adaption to highly variable conditions.

An example of the cloud classification product, covering the southern part of the Nordic area, is given by Figure 2. Different cloud and surface types are represented by different colours. An alternative presentation of the cloud classifications is demonstrated in Figure 3 where an image sequence from three satellite passages is analysed. The classifications from the two areas have here been merged into one classification with the horizontal resolution reduced to 4 km. Precipitating cloud types are shown in yellow and red colours, depending on the probabilities for light, moderate and heavy precipitation. Other cloud types are shown in different grey shades, depending on cloud altitudes.

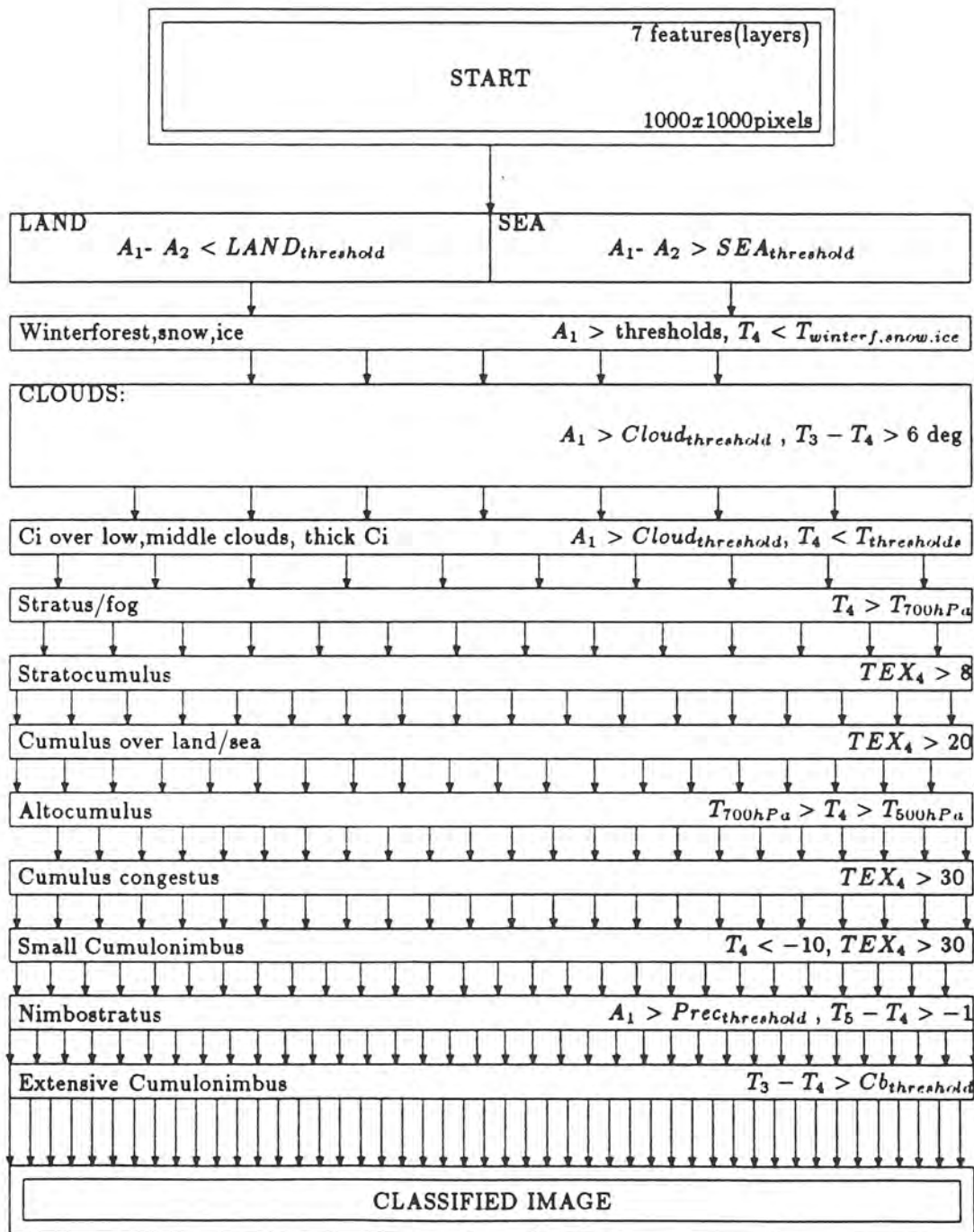


Figure 1. Simplified scheme of the steps in the classification procedure during spring with a high sun elevation. See text for a detailed explanation.

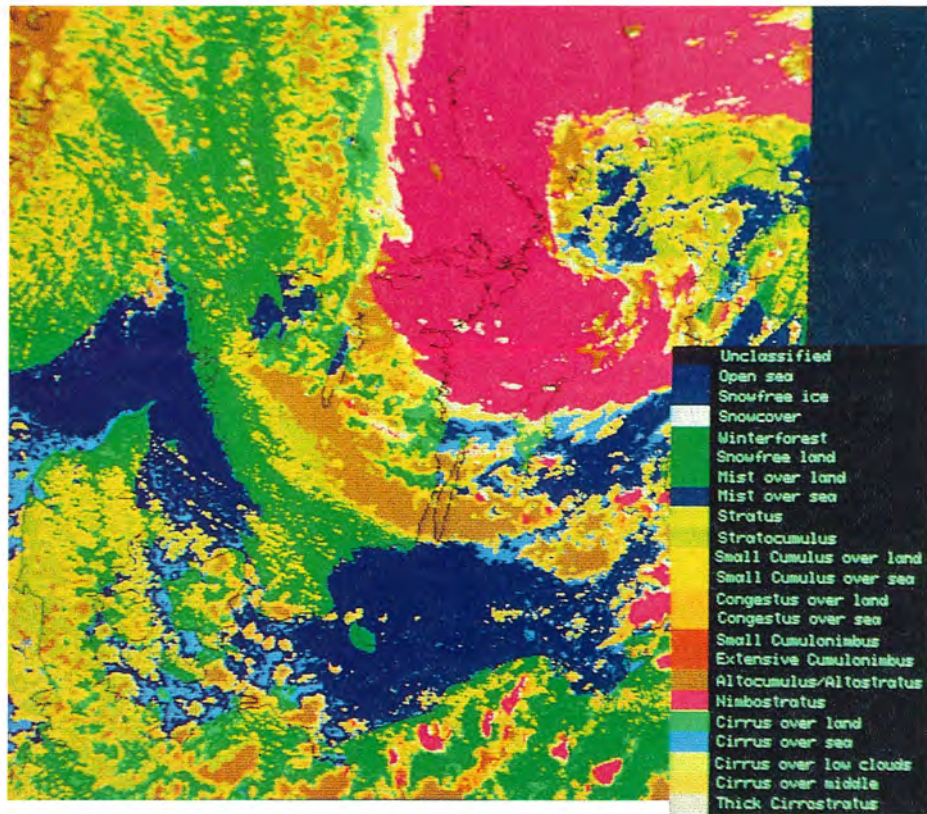


Figure 2. Cloud classification of NOAA-11 AVHRR scene 28 July 1992 12:45 UTC.

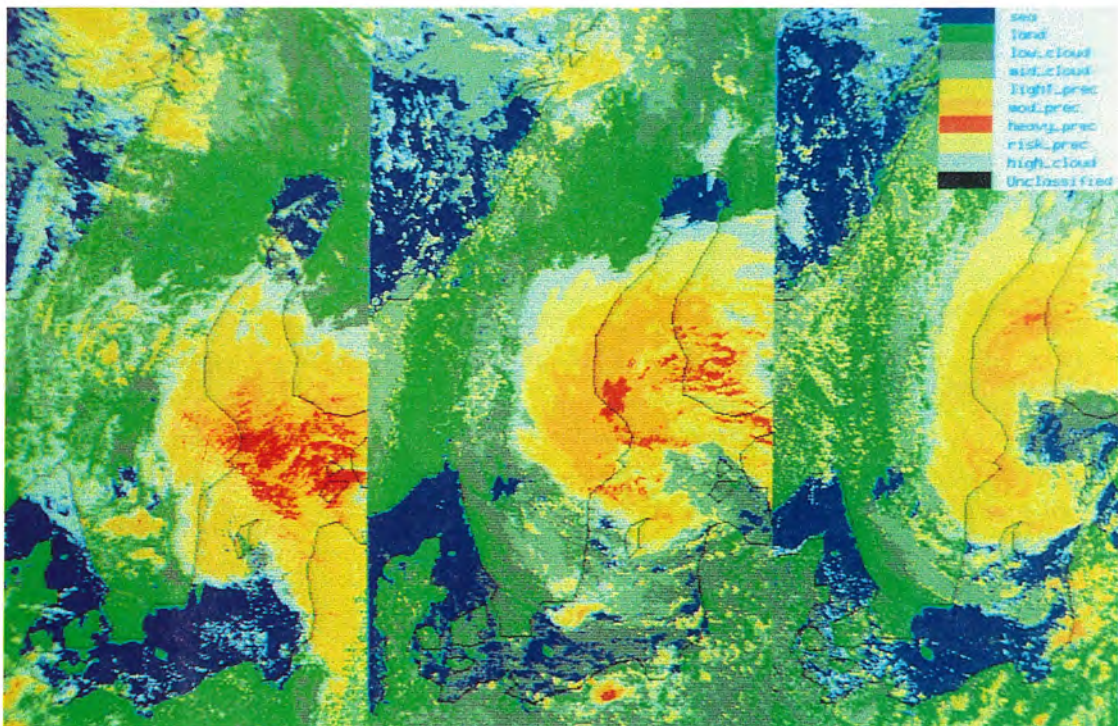


Figure 3. Sequence of cloud classifications for three AVHRR scenes 28 July 1992. Horizontal resolution reduced to 4 km. From left to right: 02:50 UTC, 08:21 UTC and 12:45 UTC.

### 3. QUALITY OF SATELLITE-DERIVED CLOUDINESS

#### 3.1 Comparison with surface observations

The idea of trying to estimate monthly cloud frequencies (described later in Section 4) from SCANDIA cloud classifications emanated from a verification study where satellite-derived cloudiness was compared with surface observations (Karlsson, 1993). Observations of total fractional cloud cover from 12 SYNOP stations were compared to satellite observations during a two-year period (15 May 1991 - 20 June 1993). The chosen SYNOP stations were located mainly at major airports where high quality cloud observations are performed more frequently (observing every hour) than at ordinary SYNOP stations (observing every third hour). A maximum time-difference of 20 minutes was allowed between a surface observation and a satellite passage. This maximum time-difference was found appropriate to minimize errors due to time-differences without reducing the amount of available observations severely. Almost 3000 satellite scenes passed the criteria for comparison with SYNOP during the period, which means that approximately 40% of all theoretically available scenes were utilized.

Surface-made cloud observations (total cloud cover) were simulated from cloud classification images by using the derived cloud information at the position and in the surrounding vicinity of each SYNOP station. Some compensation for geometrical viewing effects was adopted. The geometrical considerations for the simulation of a surface observation are schematically described in Figure 4. Low-level cloudiness was

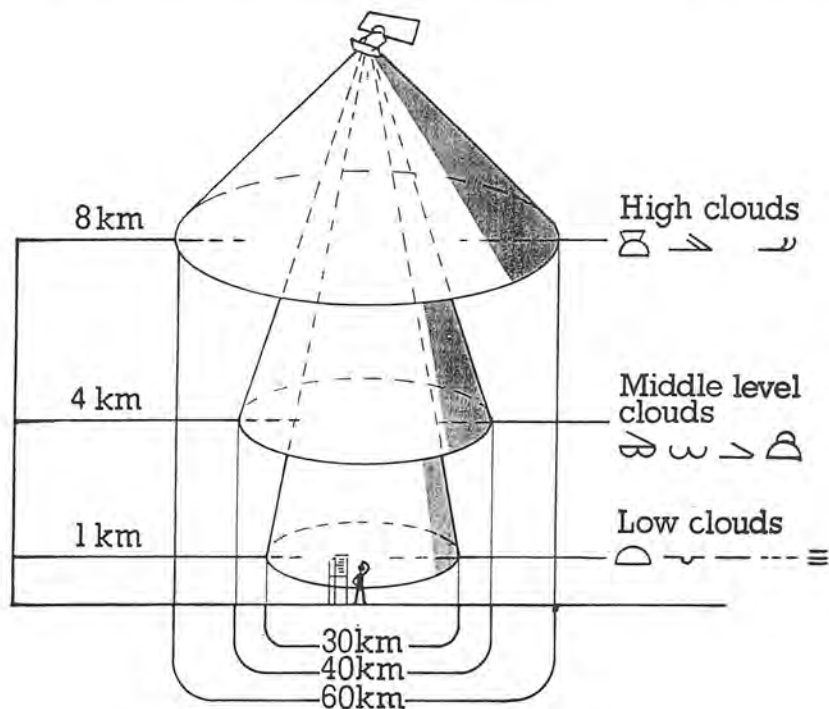


Figure 4. Simulation of surface-made cloud observations from satellite cloud classification images. See text for a detailed explanation.

estimated within 15 km radius, mid-level cloudiness within 20 km radius and high-level cloudiness within 30 km radius. The principle of random overlap was used and a larger weight was put to clouds within the smaller radii. The weighting resulted from calculations of the effective solid angles occupied by idealised clouds at three standard levels in each of the three areas (indicated in Figure 4 and described in more details by Karlsson, 1993). Notice that both the vertical and the horizontal scale in Figure 4 are highly exaggerated for clarity.

### 3.2 Results for the total comparison data set

Table 4 summarizes the results of the comparison, based on all data (23 399 comparisons between satellite and SYNOP), in a contingency table. A direct comparison in octas between satellite and SYNOP data was originally made. However, when considering the highly variable accuracy of SYNOP cloud observations (due to their subjective nature and the difficulties at night), a subdivision into a few cloudiness categories was found more appropriate here. These are: Sky Clear (denoted SKC, 0 octas), Scattered (denoted SCT, 1-4 octas), Broken (denoted BRK, 5-7 octas) and Overcast (denoted OVC, 8 octas).

The perfect match between satellite and SYNOP cloudiness is given by the diagonal in Table 4. However, we must also consider the fact that the SYNOP observer must report one octa as soon as one single cloud element can be seen. In the same way, the SYNOP

*Table 4. Contingency table comparing SYNOP-reported total cloud cover (to the left) with satellite-estimated total cloud cover (at top) for a two-year period. Cloudiness categories are defined in text.*

SAT SYNOP	SAT SKC	SAT SCT	SAT BRK	SAT OVC	$\Sigma$ SYNOP
SYNOP SKC	699	500	128	44	1371
SYNOP SCT	2366	2921	1765	348	7400
SYNOP BRK	173	1289	5672	1618	8752
SYNOP OVC	41	362	3551	1922	5876
$\Sigma$ SAT	3279	5072	11 116	3932	23 399

observer must report seven octas as soon as a single hole in the cloud deck is indicated. We may therefore include the categories SYNOP SCT + SAT SKC and SYNOP BRK + SAT OVC among the acceptable categories to compensate for these effects. When doing this, we find that 65% of all cases are now among acceptable categories while the remaining 35% seems to be subject to either under-estimation or over-estimation in the satellite observation.

Figure 5 shows RMS errors and mean errors for all four satellite categories compared to SYNOP. RMS errors larger than 2.5 octas are found for low cloud amounts while higher cloud amounts have values below 2.0 octas. Although significant variability is indicated, we must bear in mind that rounding off errors and the subjectivity of manmade cloud observations make RMS errors below 1.0 octas hardly achievable. Furthermore, geometrical differences in the way the observer and the satellite view clouds should also contribute to differences between SYNOP-reported and satellite analysed cloudiness (see later discussion). However, the large mean errors for the cloud-free (SKC) and overcast (OVC) categories in Figure 5 imply that there is a significant amount of overestimation of low cloud amounts as well as an underestimation of high cloud amounts.

### 3.3 Results for data with low satellite zenith angles

A large part of the overestimation of low cloud amounts was found to be connected to situations with high satellite zenith angles. Furthermore, the overestimation was almost dominating the results in situations when the satellite was viewing towards the rising or setting sun. A significant anisotropic enhancement of visible radiances from almost all surfaces in the scene was then causing severe problems for the cloud classifier.

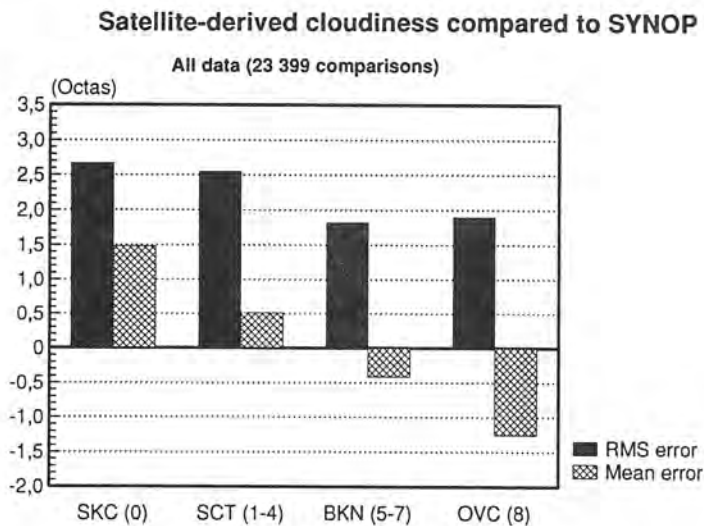


Figure 5. RMS and mean errors for satellite-simulated cloud observations compared to SYNOP. Based on data from a two-year period.

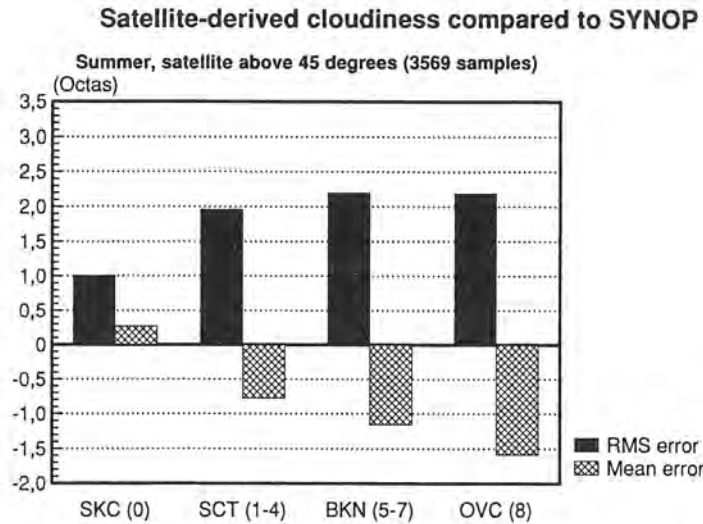


Figure 6. RMS and mean errors for satellite-simulated cloud observations compared to SYNOP. Valid in summer for satellite zenith angles below 45°.

Significantly improved results were found when excluding all satellite scenes having satellite zenith angles above 45°, especially for the summer half of the year. Figure 6 shows RMS errors and mean errors for the summer season (in this context defined as 15 May - 15 September). Here, errors have been reduced significantly for low cloud amounts and the fraction of acceptable observations have now increased to 71%. However, the underestimation of high cloud amounts seems to have increased instead.

### 3.4 SYNOP overestimation of cloudiness in summer

The underestimation of high cloud amounts in summer is believed to be caused primarily by the problem for the surface observer to estimate the total fractional cloud cover correctly in situations with low-level convective Cumulus clouds. The towering Cumulus clouds hide cloud-free areas between cloud elements when the observer views clouds at increasing zenith angles. This leads to an overestimation of cloud amounts. In addition to the perspective-induced error, a general subjective overestimation of scattered cloudiness may also contribute.

The results shown in Figure 7 support the suggestion of an overestimation of cloudiness from SYNOP. Satellite RMS and mean errors are given here as a function of the SYNOP-reported cloud amount, restricted to cases when only Cumulus clouds are observed for satellite zenith angles below 45°. Such an overestimation should be more pronounced for higher cloud amounts which is clearly indicated in Figures 6 and 7. The negative bias increases with SYNOP-reported cloud amounts, reaching a maximum level of approximately 1.5 - 2 octas for cloud amounts 5 - 8 octas. The RMS error seems to be totally dominated by the bias and an adjusted RMS error (with subtracted bias) should give RMS errors less than one octa. The use of a median-filter to remove isolated pixels (often due to spurious noise) in the classification result might lead to a slight

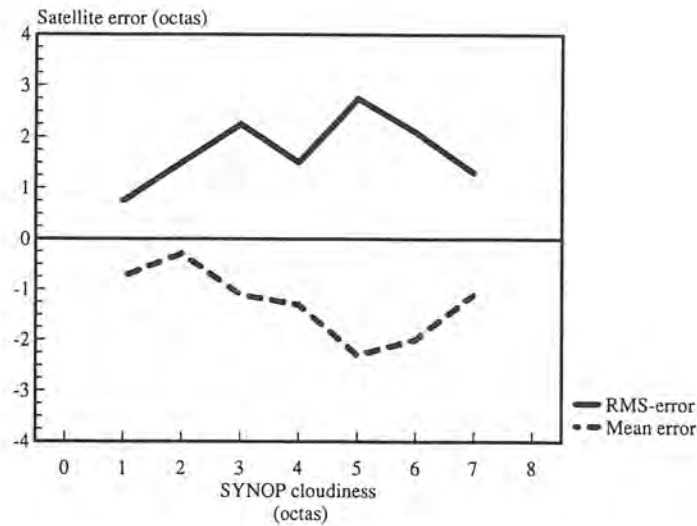


Figure 7. Same as figure 6 but for summer conditions when only low level cloud types are reported. See text for details.

underestimation of low cloud amounts in the satellite data, thus partly explaining satellite-SYNOP differences for low cloud amounts. On the contrary, the median filter should marginally increase satellite cloudiness for high cloud amounts which means that satellite-SYNOP differences would be even larger than noticed for high cloud amounts. Visual inspection of cloud classification images, in cases with large discrepancies between satellite and SYNOP cloud amounts, favoured also strongly the satellite data. We may then suggest that cloud observations from satellite during summer are even better in quality than the objective verification scores have shown here.

The bias of SYNOP cloud observations is well known. Attempts to compute solar radiation at the surface, based on radiation transfer models and SYNOP observations, have been forced to compensate for this overestimation of cloud amounts (Hoyt, 1977).

### 3.5 Results for the winter season

Figure 8 shows RMS errors and mean errors in winter (defined here as 15 November - 15 March) at satellite zenith angles below  $45^\circ$ . Errors are still relatively high here (especially RMS errors), despite the restriction to low satellite zenith angles, and the percentage of acceptable categories falls down to about 64%. The problem of underestimating high cloud amounts in winter was found to be related mainly to conditions after sunrise and before sunset (sun elevations  $2 - 6^\circ$ ). Figure 9 shows RMS errors and mean errors when conditions are restricted to the sun elevation  $2 - 6^\circ$ . A severe underestimation of low level cloudiness occurs in these situations. It is caused by the dramatic change in the spectral signature of low level water clouds in feature three (see Table 2) when changing from dark night to daylight conditions. These clouds appear colder in AVHRR channel three than in AVHRR channel four at night. The opposite is true for daylight conditions because of water clouds being able to reflect solar radiation in AVHRR channel three. The difference between the two AVHRR

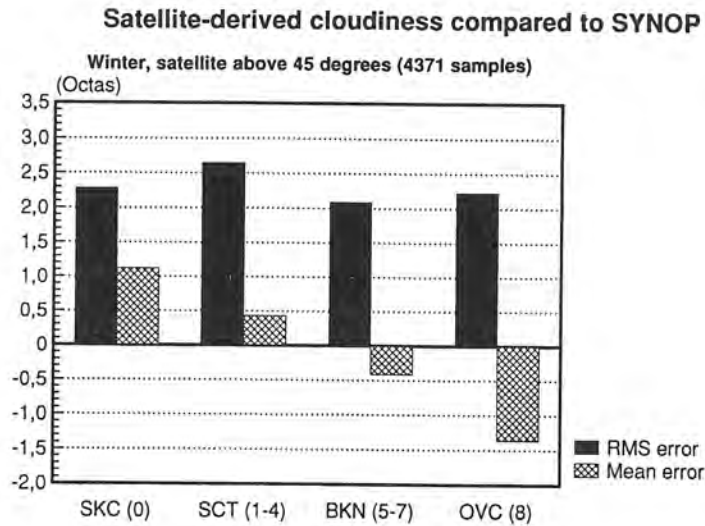


Figure 8. Same as Figure 6 but for winter conditions. See text for details.

channels for low level water clouds disappears almost entirely at sun elevations between 2 - 6°. It leads to a spectral resemblance to cloud-free areas (land and sea do not reflect significantly in AVHRR channel three, except for sunglints) and a misclassification can occur. A similar underestimation can be caused at night when thin Cirrus clouds are superimposed on top of low level water clouds. The Cirrus clouds (normally appearing warmer at night in AVHRR channel three than in AVHRR channel four for a single layer cloud) then neutralize the typical water cloud signature making it hard to separate the pixel from a cloud free pixel. Thus, this effect can contribute to the found underestimation of cloudiness in winter situations. Such an under-estimation can, of course, also occur in other seasons. However, completely dark night-time conditions and very low sun-elevations are much more frequent in the winter season that should lead

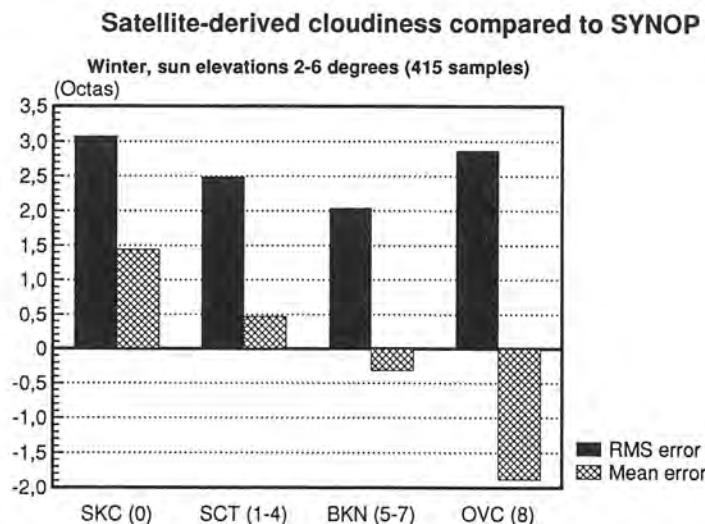


Figure 9. Same as in Figure 6 but for winter conditions with sun elevations between 2 - 6°.

to the most serious problems of this kind in winter. Figures 8 and 9 indicate also a significant overestimation of cloudiness at very low observed cloud amounts in winter. This can be explained by the confusion of cloudfree, very cold land surfaces with mid- and high-level clouds (with ice crystals and/or with mixed water droplets and ice crystals). The error was often further enhanced by a time-varying noise pattern inherent in AVHRR channel three images (Dudhia, 1989).

The increasing errors in winter may seem serious but we must also keep in mind that we have here compared with a much larger fraction of SYNOP observations made in darkness. This fact must lead to decreasing quality of the SYNOP observations. Several SYNOP observations reporting cloudfree conditions at night were often found to be completely missing Cirrus clouds that were evident in corresponding satellite images.

### 3.6 Distribution of absolute errors

Finally, another way to summarize the results is to divide the material into groups having different absolute errors. We define four such groups: 0 - 2 octas, 2 - 4 octas, 4 - 6 octas and 6 - 8 octas. The first group may be seen as the group representing quite an acceptable error. This can be concluded when considering possible sources of error related to the used comparison method and the inherent errors of the SYNOP observations. The two last groups would then contain the worst cases, i.e. when cloudiness is severely overestimated in almost cloudfree conditions and when cloudiness is severely underestimated in cloudy conditions. Table 5 shows the verification results for the following six situations:

- a) Sun elevations above 10°.
- b) Sun elevations between -5° and 10°.
- c) Night conditions.
- d) Summer conditions (15 May - 15 September).
- e) Winter conditions (15 November - 15 March).
- f) All data (15 May 1991 - 20 June 1993).

Table 5. Total distribution of absolute error categories, in % of all studied cases, for conditions a-f (explained in text).

Absolute error category	a)	b)	c)	d)	e)	f)
0-2 octas	86.0%	78.3%	78.5%	83.6%	78.1%	81.4%
2-4 octas	10.5%	14.0%	13.9%	12.8%	13.0%	12.6%
4-6 octas	3.1%	5.8%	5.8%	3.1%	6.5%	4.7%
6-8 octas	0.4%	1.9%	1.8%	0.5%	2.3%	1.3%
Σ samples	9 352	6 764	7 283	7 164	8 658	23 399

The good results for the summer half of the year are again confirmed, especially when the sun is at high elevations. Results are worse at night, at very low sun elevations and in winter. However, the fraction of acceptable observations is still as high as 78% for these categories which indicates that large errors seem to occur only in exceptional cases.

### 3.7 Conclusion of the verification study

Despite the above discussed defects, satellite-derived cloud information from SCANDIA seems to be of particularly good quality for scenes with low satellite zenith angles. It means in practice that at least four high quality cloud observations per day are available in the Nordic region from the two existing NOAA-satellites. Furthermore, these observations have an exceptionally high spatial resolution (at maximum 1.1 km) compared to the spatial distribution of surface observing SYNOP stations (approximately 40 - 100 km for land areas). The satellite observations are also covering large sea areas where surface observations are extremely sparse, both in time and space. These findings led to the attempt to use results from SCANDIA to describe mean cloud conditions for the entire year of 1993.

## 4. COMPUTATION OF MONTHLY CLOUD FREQUENCIES

All available satellite passages, received in 1993 at SMHI in Norrköping, with minimum satellite zenith angles below 45° at reception, were selected for this study. Generally, this meant that four satellite scenes were used each day to describe cloud conditions in Sweden and its close surroundings. The chosen satellite scenes, with the present satellites NOAA-11 and NOAA-12, describe roughly cloud conditions during early morning, morning, afternoon and evening. The sun-synchronous orbits of the current satellites guarantee at least one passage with satellite zenith angles below 45° within the approximate time-windows shown in Table 6.

*Table 6. Approximate time-windows valid for the used satellite scenes from NOAA-11 and NOAA-12 in 1993. At least one passage with low satellite zenith angles is guaranteed within a time-window each day.*

Time of day	Time-window (UTC)	Satellite
Early morning	03:00 - 05:00	NOAA-11
Morning	06:30 - 08:30	NOAA-12
Afternoon	13:00 - 15:00	NOAA-11
Evening	16:30 - 18:30	NOAA-12

Cloud analyses from SCANDIA were treated in the following way:

- a) Each pixel in the high resolution classification image was labelled cloudy or cloudfree depending on the resulting cloud and surface types. Pixels classified as subpixel clouds (see Table 3) were treated as cloud-free.
- b) A resampling of the result image by a nearest neighbour resampling technique was done to reduce the nominal horizontal resolution from one to four km.
- c) Classification results for the two areas (mentioned in Section 2) were merged into one result image (covering the same area as in Figure 3).
- d) Cloud frequencies for an entire month were finally estimated by calculating the fraction of the total available scenes where the pixel was labelled as cloudy. For example, 20% means that the pixel was classified as cloudy in 20% of all used images in a month (normally approximately 120 images).

The reduction of the horizontal resolution can be motivated by the fact that geometrical errors of the order of 2 - 5 km are probably present in the satellite images (e.g. discussed by Borders *et al.* (1992)). Such errors are introduced by uncertainties in used orbital information and satellite passage times when automatically transforming images from satellite projection to any map projection. Some problems with NOAA-receptions occurred occasionally in 1993 and Table 7 shows the fraction of the theoretically available scenes that were used in this study.

Besides restricting the used satellite scenes to only scenes with low satellite zenith angles, all used classification images were visually inspected to remove any possible corrupt scenes due to production problems. A few very problematic scenes in situations near sunrise or sunset (as discussed in Section 3) were also removed from the data in November and February during this quality control process.

## 5. CLOUDINESS IN 1993

This section presents satellite-derived cloud frequencies for all months in 1993. Each month is discussed separately in Section 5.1 where results are related to the dominating weather patterns. Results are also compared to corresponding estimations of mean cloudiness from SYNOP observations (SMHI, 1993-1994). High resolution (4 km) cloud frequencies are shown in colour-coded 10% intervals by figures 15 - 18 on pages 23 - 26. Figures, comparing satellite observations with SYNOP observations, can be found in the Appendix. Here, monthly cloud frequencies from satellite have been reduced in horizontal resolution from 4 km to 20 km (by computing areal means) and they are represented by various levels of hatchings and isolines. SYNOP-based estimations of mean cloudiness (in %) over the Swedish area are presented as manually analysed isoline maps for all months in 1993. The computation of mean cloudiness from SYNOP was carried out by using observations at 06, 12 and 18 UTC. This is quite comparable

*Table 7. Number of used satellite scenes compared to the theoretically available for each of the studied months in summer 1993. Four scenes per day are requested for 100% daily coverage.*

Month	Number of used scenes	Fraction of theoretically available scenes (%)
January	99	79.8
February	104	92.9
March	116	93.5
April	120	100.0
May	116	93.5
June	117	97.5
July	113	91.1
August	119	96.0
September	100	83.3
October	99	79.8
November	107	89.2
December	117	94.4
Year 1993	1 327	90.9

to the way cloud frequencies have been estimated from the satellite information (see Table 6). However, one difference is that the satellite data also consist of early morning observations in addition to morning, afternoon and evening observations.

Section 5.2 presents and discusses the satellite-derived annual mean of cloud frequencies in 1993. High resolution (4 km) annual cloud frequencies are shown on the front cover in colour-coded 5% intervals. A comparison of satellite-derived and SYNOP-derived annual cloud frequencies is given in Section 5.2 in the same manner as in the Appendix. Results are furthermore compared to analyses of accumulated sunshine duration based on measurements from a network of automatic and manual stations.

Finally, a study of the diurnal variation of satellite-derived cloud frequencies is given in Section 5.3. Cloud conditions at the four daily satellite observation occasions are compared for June and for December.

## 5.1 Monthly cloud frequencies

### 5.1.1 January

The year of 1993 started with a warm and very windy January. The monthly mean of sea level pressure (shown in Figure 10) reveals a strong, dominating southwesterly wind pattern. Such a weather type, connected with rapidly passing intense extra-tropical cyclones over Scandinavia, apparently causes high cloud frequencies (60 - 75%) in the western part of the area and a well-defined minimum in cloud frequencies (35 - 50%) along the Swedish eastern coastline. We may suggest that this is caused primarily by orographic effects induced by the Scandinavian mountain range.

The same cloudiness pattern can be found in the SYNOP analysis (Appendix page 3), but some differences can be noticed. The most pronounced difference is the SYNOP maximum of approximately 70% in the inner part of southern Sweden. Satellite data show values of only 45 - 60% here. This difference is explained to some degree by a loss of a large part of the satellite scenes this month (see Table 7). However, a large part of the discrepancy is explained by the underestimation of low level cloudiness in the satellite information in situations with very low sun elevations (as discussed in section 4). Evidence of such an underestimation can be found in many places in the satellite analysis.

Although the satellite analysis misses the maximum in cloudiness in the southern part of Sweden, the satellite estimate strongly supports the locations of individual maxima and minima in the SYNOP analysis.

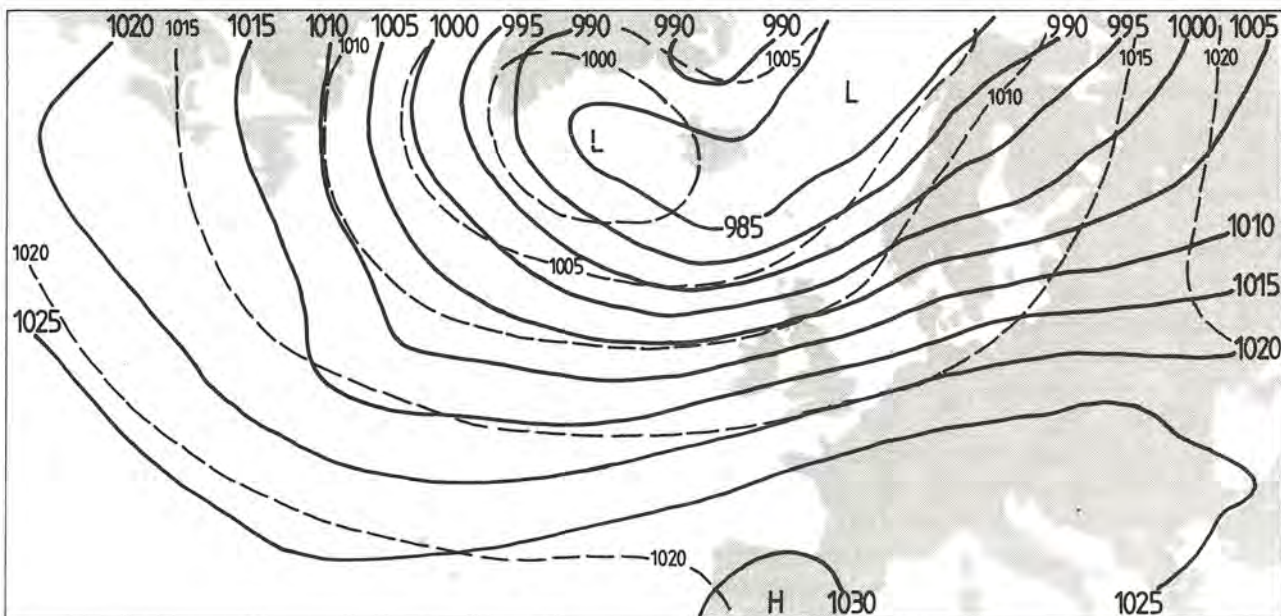


Figure 10. Mean sea-level pressure in January 1993. Solid lines show analysed value and dashed lines show climate mean (1931 - 1960).

### 5.1.2 February

The warm and windy weather type of January continued during the first two-thirds of February. The month ended with cold weather in connection with northerly winds and with an anticyclone forming over the central part. Cloud conditions are similar to the situation in January in the northern half of the area while the southern part experiences more cloudy conditions.

The agreement between the satellite and the SYNOP analyses is generally good. A displacement to the south of the SYNOP-indicated minimum in cloudiness is, however, found in the northeastern part of Sweden. We again find a slight underestimation of cloud frequencies for the southern part of Sweden. The chosen NOAA-12 passages in the morning (see Table 6) occurred in February often at sun elevations between 2 - 6°. Thus, cloud analyses are then often subject to conditions causing an underestimation of low level cloudiness.

### 5.1.3 March

The weather in March was very changeable with both anticyclonic and cyclonic periods. However, a high frequency of westerly or northwesterly winds (as shown by Figure 11) led to the formation of a distinct minimum in cloud frequencies (40 - 50%) in the central part in the lee of the Norwegian and Swedish mountains. High cloud frequencies of 70 - 80% are now found in the inner part of southern Sweden as well as in the

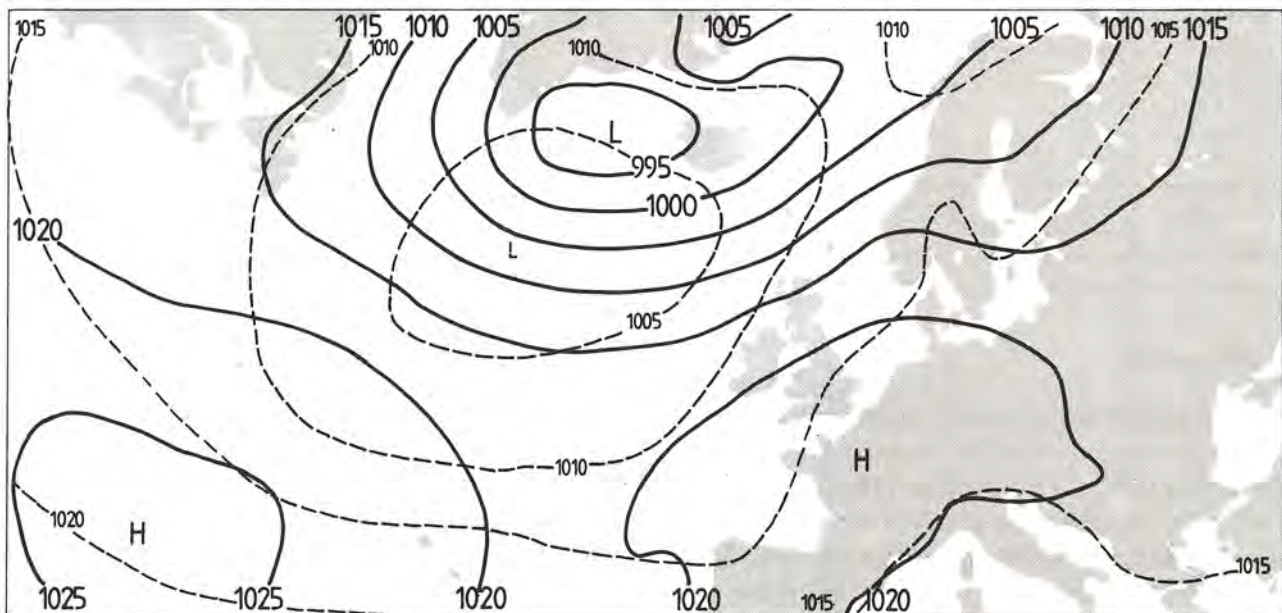


Figure 11. Mean sea-level pressure in March 1993. Solid lines show analysed value and dashed lines show climate mean (1931 - 1960).

mountain areas in the north. Outside of Sweden, high cloud frequencies (70 - 85%) are indicated in the eastern part and on the Norwegian Sea. The agreement with the SYNOP analysis is now excellent. Higher sun elevations and warmer ground temperatures seem to have improved the satellite analysis substantially.

#### 5.1.4 April

This month had changeable weather (like in March), but some stable anticyclonic periods existed. We again find a very good agreement between the satellite and the SYNOP analysis. A complete satellite data set (100% of available scenes) was available in April.

Pronounced differences between land and sea areas can be found in the satellite analysis. Cloud frequencies are typically 10 - 20 % lower over sea areas compared to those over land areas. This is most probably caused by the effect of differential heating of land and sea surfaces. Land surfaces are effectively heated during daytime, which often leads to the formation of convective Cumulus clouds. Sea surfaces, on the contrary, are not heated in the same way due to mixing processes in the sea and to the high heat capacity of water. The SYNOP analysis does support (indirectly by using observations from coastal stations) the satellite-indicated cloud situation at sea. A similar effect can be seen in both analyses near the great lakes of Vänern and Vättern. We have therefore reason to be rather confident in the satellite analysis over sea areas.

Notice in particular the distinct minimum in cloud frequencies that is indicated close to the Norwegian coast. The minimum is surrounded by high cloud frequencies in the mountains and far out over the Norwegian Sea.

#### 5.1.5 May

May was totally dominated by a strong anticyclone which persisted almost the entire month. The analysis of mean sea level pressure in Figure 12 indicates higher pressure values than normal, with weak winds in the Nordic area. Such a weather type created very low cloud frequencies, especially in the southern part and over sea areas. In many places here, monthly minimum values for 1993 are found. An absolute minimum of 15% is found in the southern part of the Baltic Sea. Cloud frequencies are higher in the mountain areas and in the northern part. This is probably caused by a closer proximity to minor low pressure systems passing over the Norwegian Sea and the Barent Sea.

The comparison with SYNOP is again showing excellent agreement. Notice in particular the local maximum in cloud frequencies in the southwestern part of Sweden and the strong gradient in cloud frequencies in the central part of the area. These features are described as very similar in both analyses.

Notice also again the minimum in cloud frequencies near the Norwegian coast, almost as pronounced as in April. It is interesting to see that the minimum is collocated with a minimum in sea surface temperatures typical for this season (see Figure 13). Similar

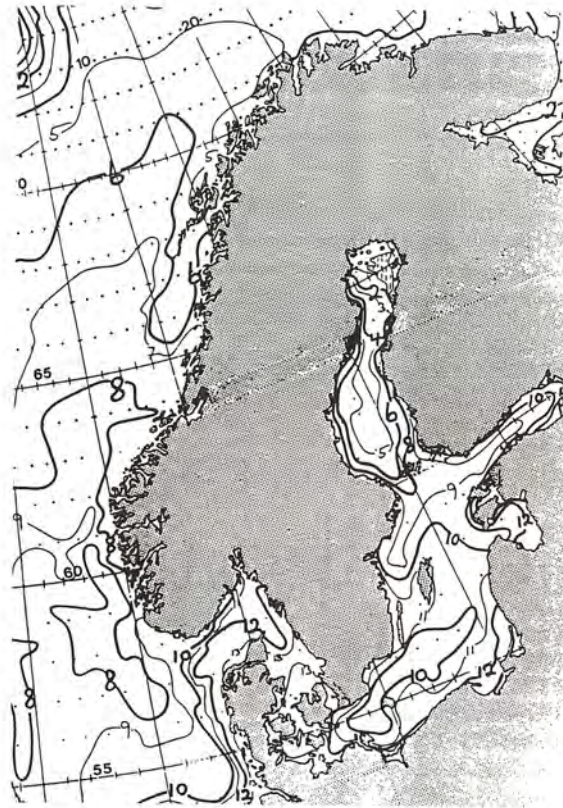


Figure 12. Sea surface temperatures ( $^{\circ}\text{C}$ ) valid between 14 - 18 May 1993. Analysis provided by the Norwegian Meteorological Institute.

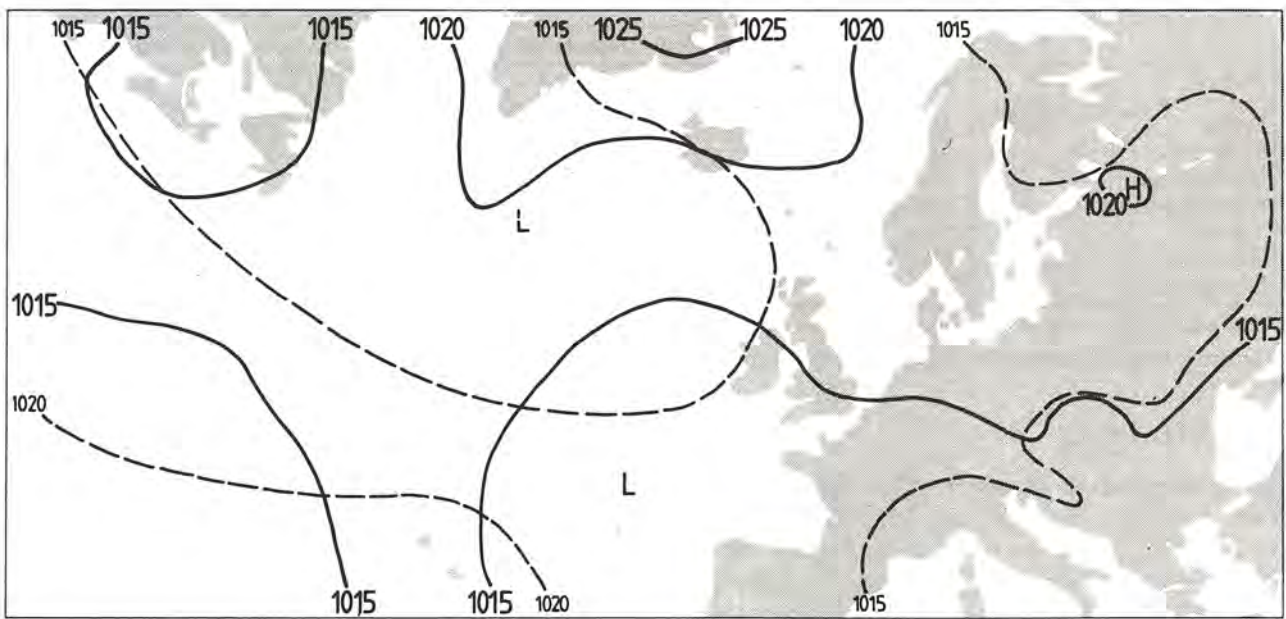


Figure 13. Mean sea-level pressure in May 1993. Solid lines show analysed value and dashed lines show climate mean (1931 - 1960).

conditions prevailed for a long period in spring and in early summer. The forcing from the slightly colder water (compared to sea areas far off the coast) combined with the proximity to the cloud-generating mountain areas seem to create conditions for reducing cloudiness substantially at this location. One might also suspect this effect to be a lee effect in a weather situation with dominating easterly winds. However, such conditions were not persistent in May.

#### 5.1.6 June

The weather type changed drastically in June to become more cyclonic. Periods with unstable air masses dominated, often in connection with northerly winds. The satellite-derived cloud frequencies show here even larger variations between land and sea areas than in May and in April. Cloud frequencies over land are generally above 50% while at sea, cloud frequencies stay between 30 - 50%. Notice especially the influences on cloud frequencies by the Gulf of Bothnia, by the lakes of Vänern and Vättern and by the island of Gotland. Very high cloud frequencies (above 80%) are found in the mountains, in the most northern parts and over the Norwegian Sea (except near the coast - the earlier discussed minimum persisted thus also in June).

The agreement is good between SYNOP and satellite, but a small underestimation of cloud frequencies is indicated again in the southern part. This is most probably caused by an overestimation of total cloud cover by the surface observer (as discussed in Section 4). It may also marginally be explained by prevailing situations with very low sun elevations at the early morning NOAA-11 passages. A third explanation is also the use of more night-time observations (often less cloudy) in the satellite analysis compared to the set of used SYNOP-observations.

#### 5.1.7 July

A strong cyclonic dominance (figure 14) caused unusually high cloud frequencies for a summer month like July. Cloud frequencies are as high as 70 - 85% in the central part of the area (collocated with the minimum in sea level pressure in Figure 14). Cloud frequencies are generally high over land areas. Only near the lake of Vänern and near the Gulf of Bothnia cloud frequencies below 60% are found over land. Minima in cloud frequencies (35 - 45 %) are found on the Åland Sea and in the Gulf of Bothnia.

The comparison with SYNOP shows again a very satisfying resemblance with the satellite analysis. Notice in particular features like the inland maximum in the inner part of southern Sweden and the minimum near the Gulf of Bothnia. We can especially notice two features in the satellite analysis (best seen in Figure 17) which are not captured by the SYNOP analysis. These are the minimum (below 60%) over the lake of Vänern and the maximum (60 - 65%) at the northeast corner of the island of Gotland. The location of this latter maximum is most probably caused by the eastward advection of clouds originally generated over Gotland. The same effect can be seen along the eastern coast of Sweden, displacing the strongest gradients in cloud frequencies eastward outside the coastline.

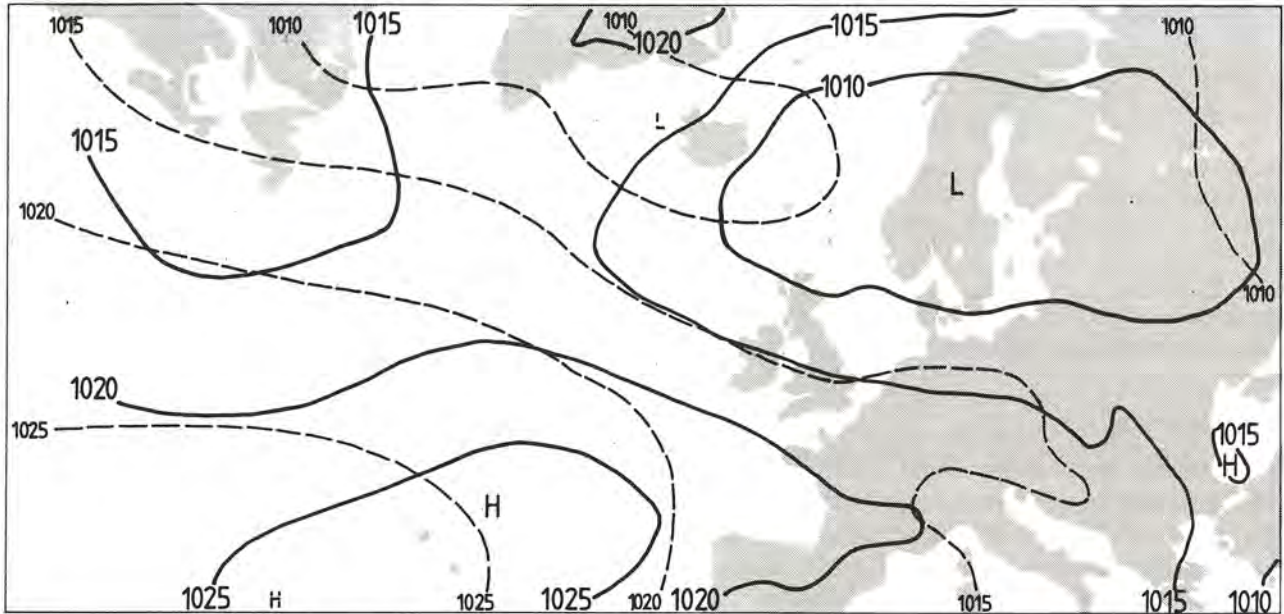


Figure 14. Mean sea-level pressure in July 1993. Solid lines show analysed value and dashed lines show climate mean (1931 - 1960).

#### 5.1.8 August

The cyclonic weather type continued in August and the resulting cloud frequencies are then quite similar to those in July. Highest cloud frequencies (80 - 90 %) are found in the mountain areas and in the northeastern part. A minimum of 35 - 40 % shows up in the southern part of the Baltic Sea. The agreement with SYNOP is still very good, but some underestimation can be seen.

We can still see that sea areas have lower cloud frequencies than land areas, but the difference is not as pronounced as earlier in the summer. The warmer sea surface temperatures (at this time 13 - 17°C) have now diminished the prohibiting effect on cloud formation at sea.

#### 5.1.9 September

September was dominated by unusually cold anticyclonic conditions (Figure 19) and long periods with easterly winds occurred. The anticyclone reduced cloud frequencies slightly in the central part of the area compared to in August. However, weather systems from central Europe occasionally influenced the weather in the southern part causing high cloud frequencies here. Frequent formation of low-level temperature inversions with accompanying Stratus clouds also contributed to the high cloud frequencies despite the anticyclonic dominance.

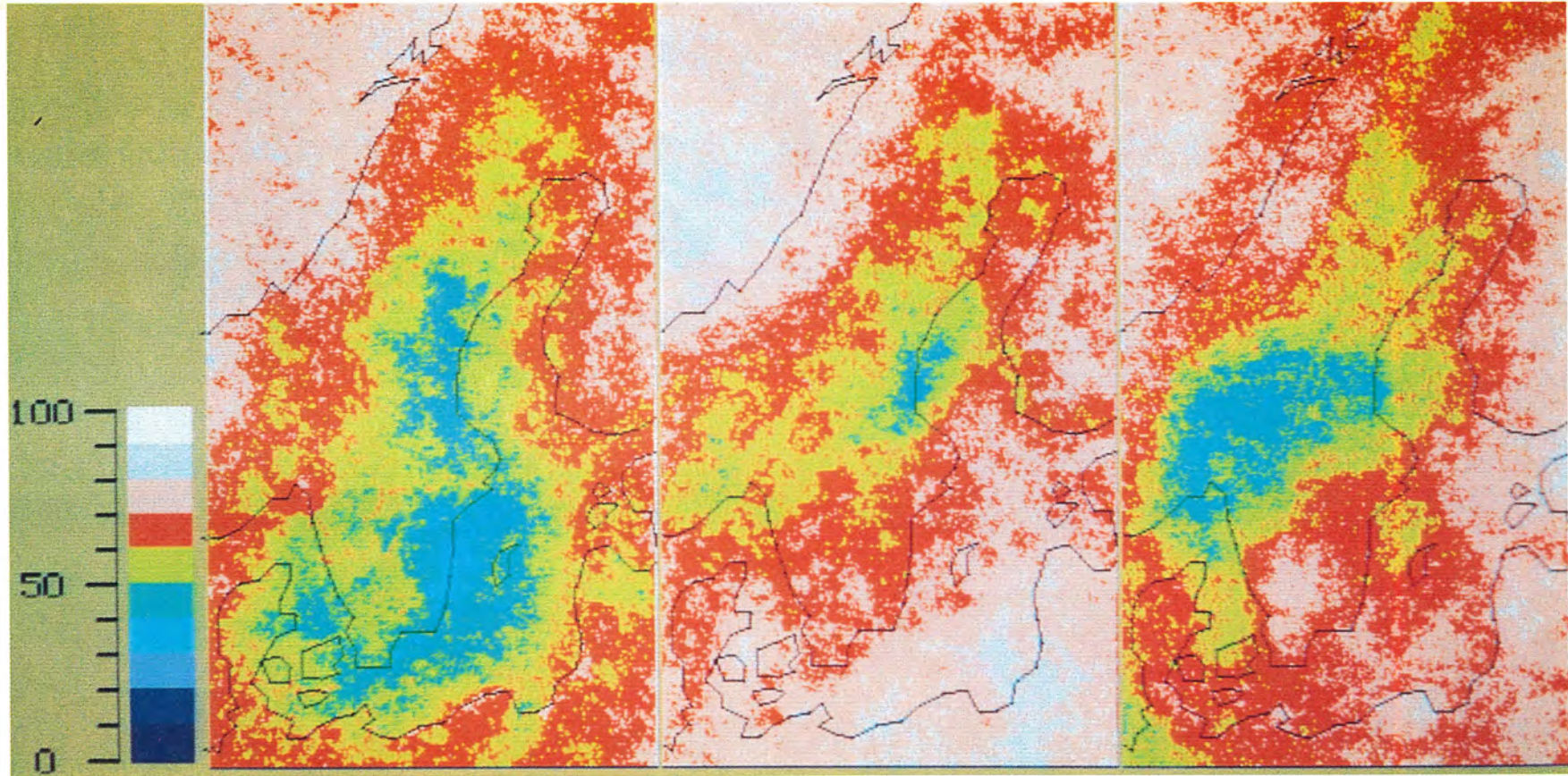


Figure 15. Satellite-derived cloud frequencies (%) in 1993 for the months of January, February and March (from left to right).

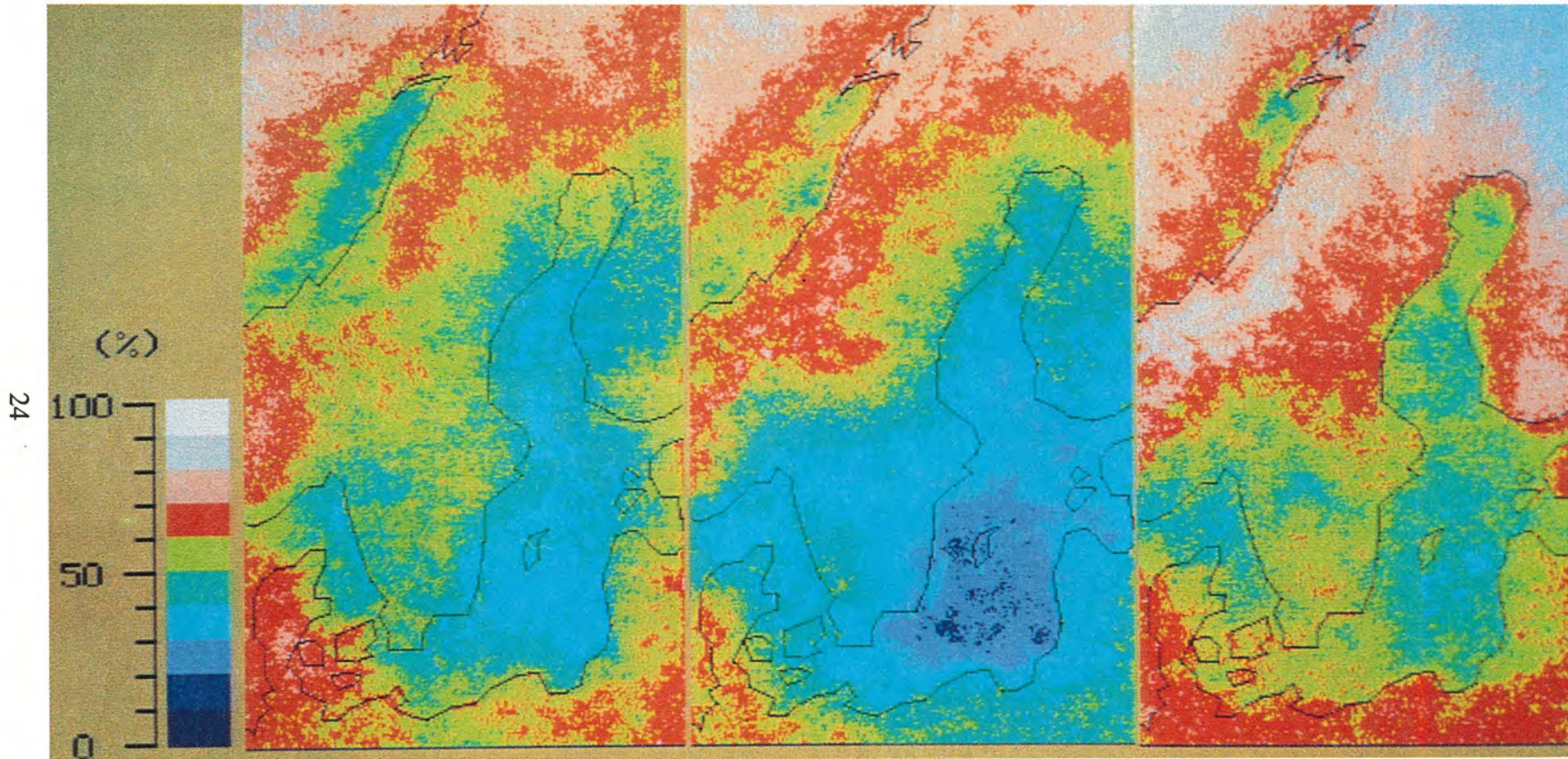


Figure 16. Satellite-derived cloud frequencies (%) in 1993 for the months of April, May and June (from left to right).

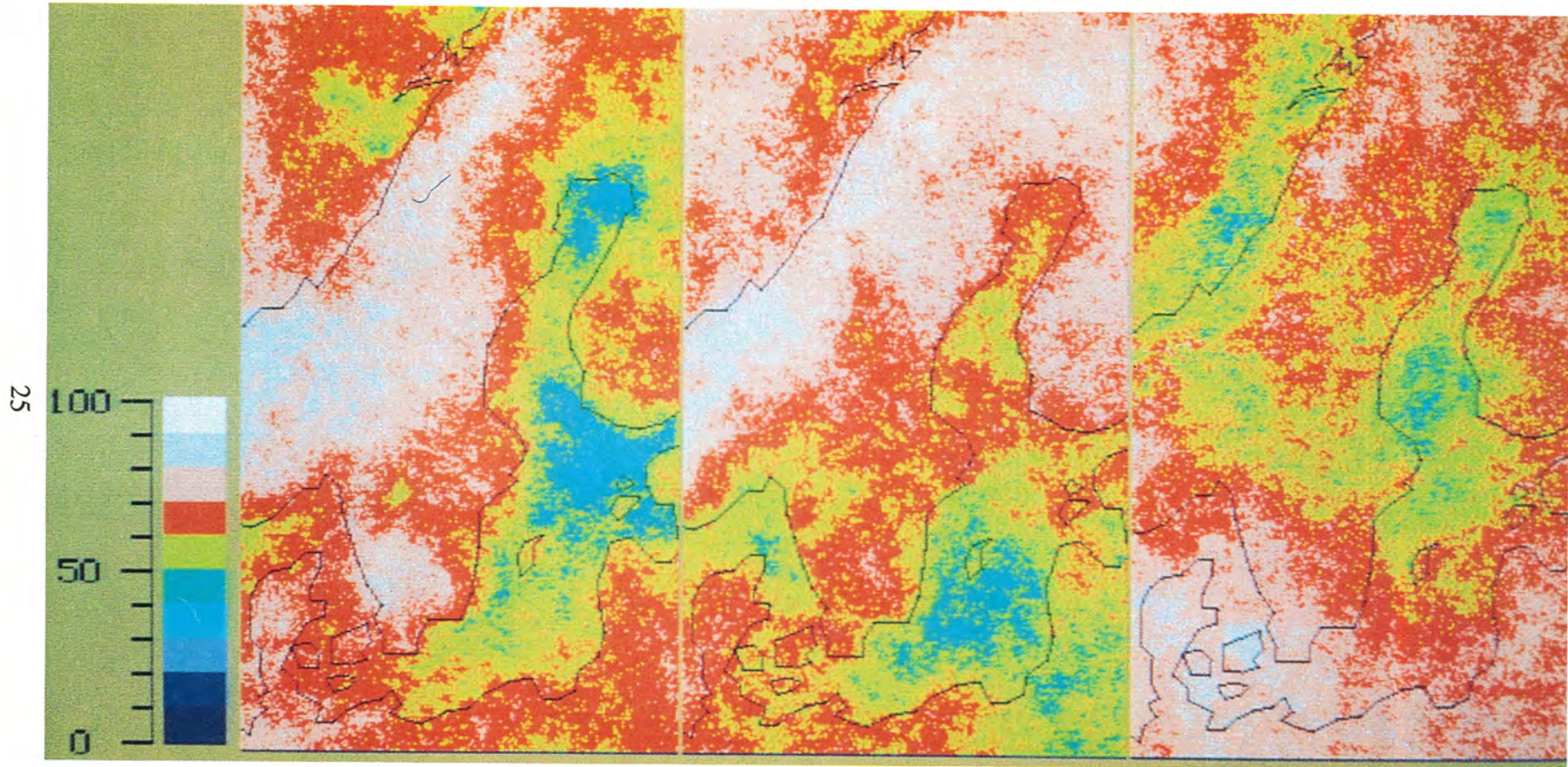


Figure 17. Satellite-derived cloud frequencies (%) in 1993 for the months of July, August and September (from left to right).

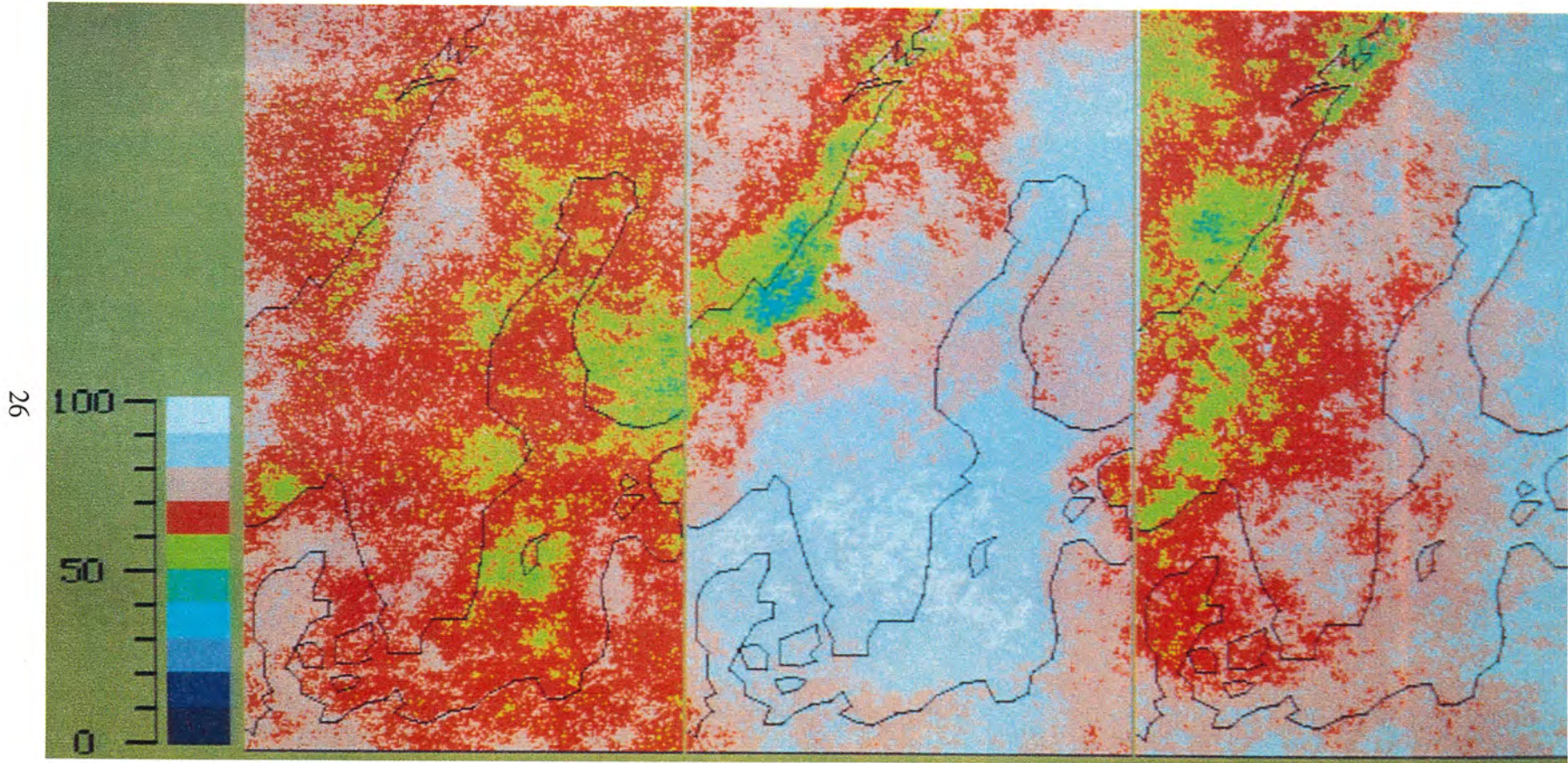


Figure 18. Satellite-derived cloud frequencies (%) in 1993 for the months of October, November and December (from left to right).

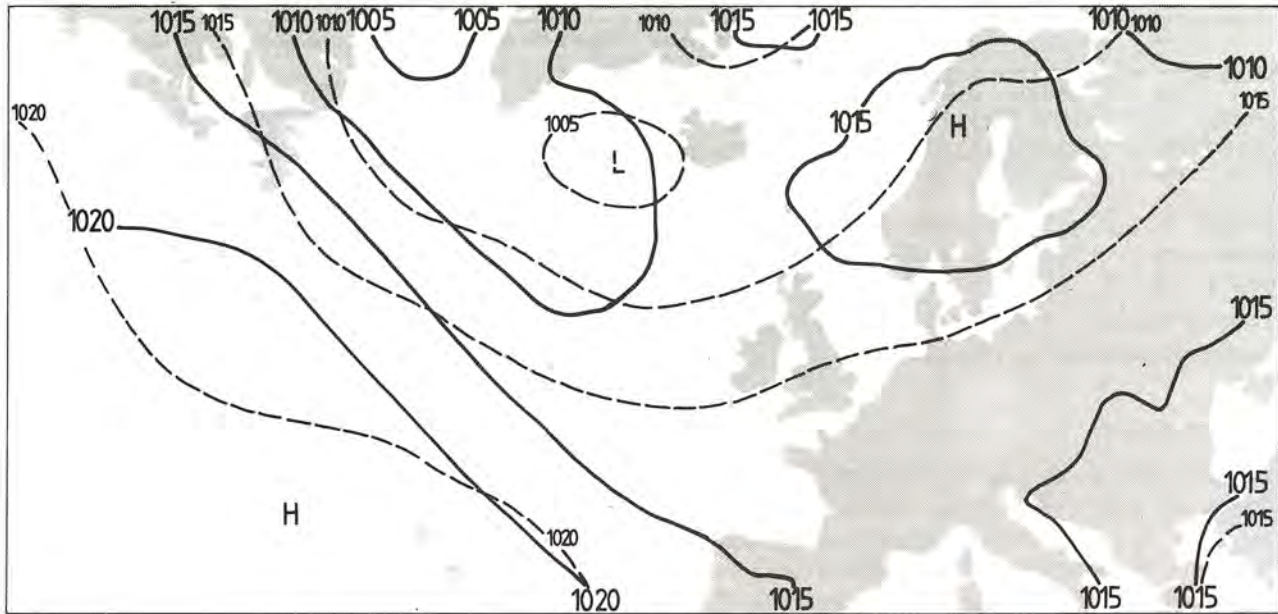


Figure 19. Mean sea-level pressure in September 1993. Solid lines show analysed value and dashed lines show climate mean (1931 - 1960).

The SYNOP analysis is again very close to the satellite analysis. Notice features like the high values in the most southern part, the low values in the central part and the local maximum in the Swedish mountains.

#### 5.1.10 October

The weather this month was very changeable and somewhat colder than normal. Satellite-analysed cloud frequencies are now high in the entire area (between 50 - 80 %) with rather small regional differences. Furthermore, there are no longer any significant differences between land and sea areas.

The loss of 20% of all available satellite scenes (see Table 7) in October is due to technical maintenance of the NOAA-12 AVHRR instrument, and it makes the satellite analysis somewhat uncertain. Nevertheless, the comparison with SYNOP still shows a very satisfying resemblance.

#### 5.1.11 November

An anticyclonic weather type dominated in November in most of the area, but the northern part was influenced by passing extra-tropical cyclones (Figure 20). Exceptionally high cloud frequencies are found over large areas this month. November was in many places the most cloudy month of 1993. Values above 90% are found frequently in southern Sweden, with the absolute maximum of 99% near Vimmerby in

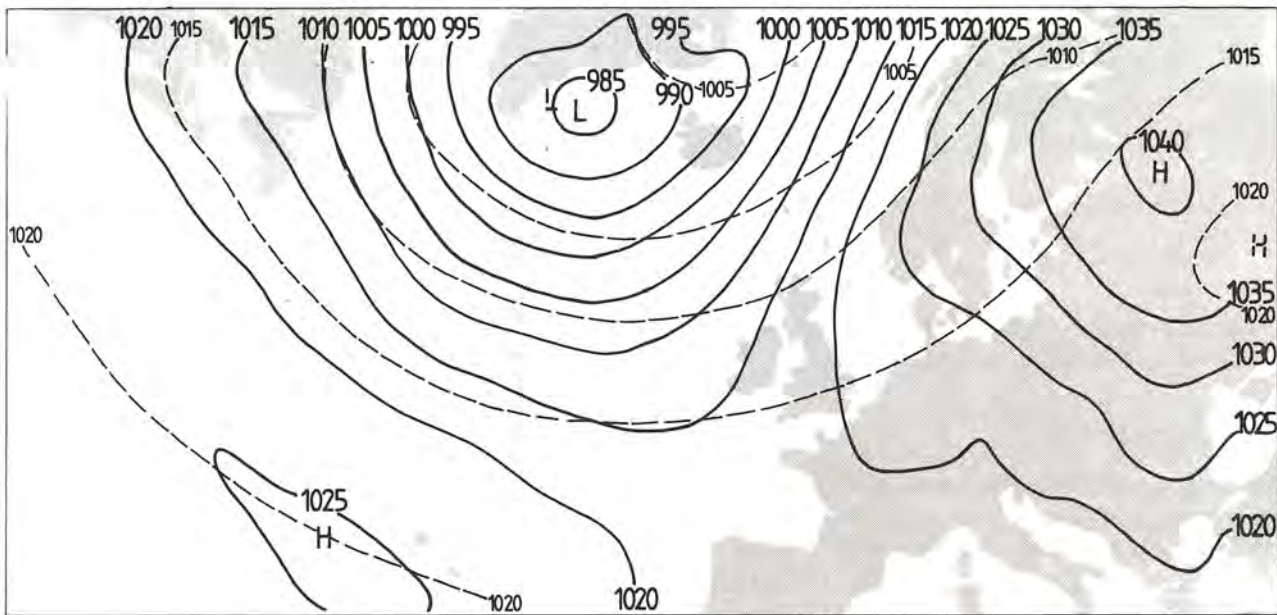


Figure 20. Mean sea-level pressure in November 1993. Solid lines show analysed value and dashed lines show climate mean (1931 - 1960).

the southeastern part. Low level clouds formed in the temperature inversions associated with the anticyclone and persisted for long periods.

Like in February, a small number (11 in total) of NOAA-12 scenes were excluded from the satellite data set. This was done to avoid some evidently bad analyses of low level cloudiness connected with low sun elevations. Again, the comparison with SYNOP generally shows a very good agreement, but some underestimation of cloud frequencies is evident.

Notice the existence of a minimum in cloud frequencies along the Norwegian coast with the lowest values (45 - 50%) near Trondheim (partly indicated in the SYNOP analysis). The minimum is most probably caused by a lee effect behind the mountains due to the dominating southeasterly winds (see Figure 20).

#### 5.1.12 December

December had a more cyclonic weather type with a series of extra-tropical cyclones passing from the southwest. In addition, low-level Stratus clouds were frequent, thus leading to relatively high cloud frequencies. The satellite analysis shows values between 60 - 80 % for most of the area, except for the mountain areas and parts of the Norwegian Sea.

A good resemblance between the satellite and SYNOP analysis is at hand, except for a small but evident underestimation in the satellite data.

## 5.2 Annual mean of cloud frequencies for 1993

An annual mean of cloud frequencies has been computed by averaging the results from all months in 1993. The result is shown on the front cover where cloud frequencies are colour-coded into 5% intervals. Figure 21 shows (in the left part) the same analysis but with the horizontal resolution reduced to 20 km (by computing areal means). It can be compared to the corresponding analysis based on SYNOP observations to the right in Figure 21. The SYNOP analysis was computed from the data for individual months shown in the Appendix.

Naturally, the annual mean is not showing the same regional variability as in individual months. Cloud frequencies are generally restricted to 50 - 80%. Regional differences are nevertheless very evident. We can see that the earlier found low cloud frequency over sea areas in summer is clearly discernible also in the annual mean. The absolute minimum of 53% is found in the Baltic Sea between Gotland and the Swedish mainland. Lowest cloud frequencies over Swedish land areas are found near the eastern coast, over Gotland and near the lakes of Vänern and Vättern. Highest cloud frequencies (above 70%) are found in the mountains, in the northern parts of Sweden and Finland

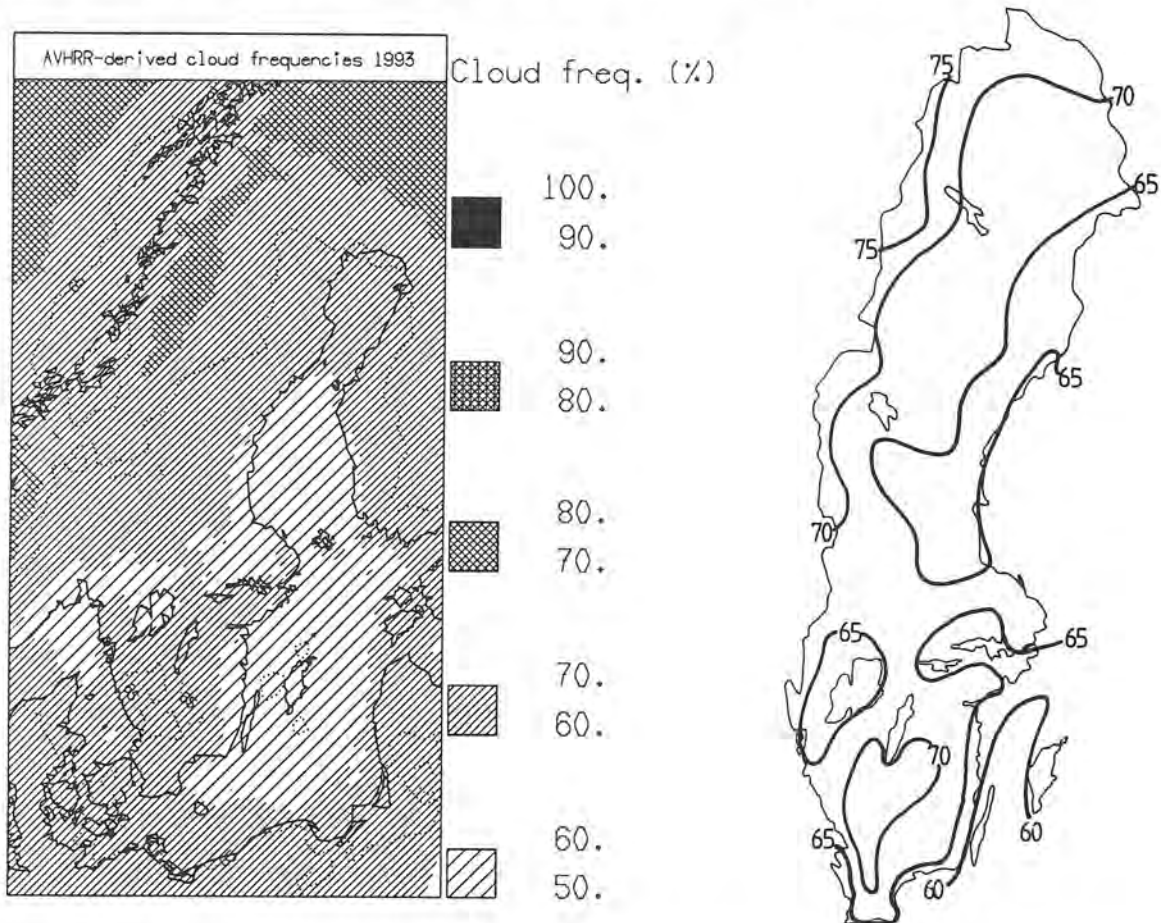


Figure 21. Satellite-derived annual mean of cloud frequencies (%) in 1993 (left) and corresponding analysis of mean cloudiness from SYNOP (right).

and far out over the Norwegian Sea. The absolute maximum in the studied area is 80% and it is located in the most northern part of the Scandinavian mountains (on the Norwegian side). An interesting local maximum of 65 - 70 % is also found in the inner part of southern Sweden. Notice also the minimum in cloud frequencies that can be seen in the Norwegian Sea close to the Norwegian coast (discussed in detail in Section 5.1.5).

The comparison with SYNOP in general gives good agreement with the satellite analysis. However, SYNOP cloud frequencies are somewhat higher. It is most clearly seen for the local maximum in the inner part of southern Sweden. The underestimation of cloudiness, especially for the winter months (found earlier in Section 5.2 and discussed in Section 4), is thus noticeable but small in the satellite-estimated annual mean.

It is interesting to notice that the manual analysis in Figure 21 (to the right) does not indicate a minimum in cloud frequencies offshore in the Bothnian Sea. Instead, an inland minimum is analysed here. We suggest that the use of only a few SYNOP stations combined with the lack of sea observations is responsible for these differences.

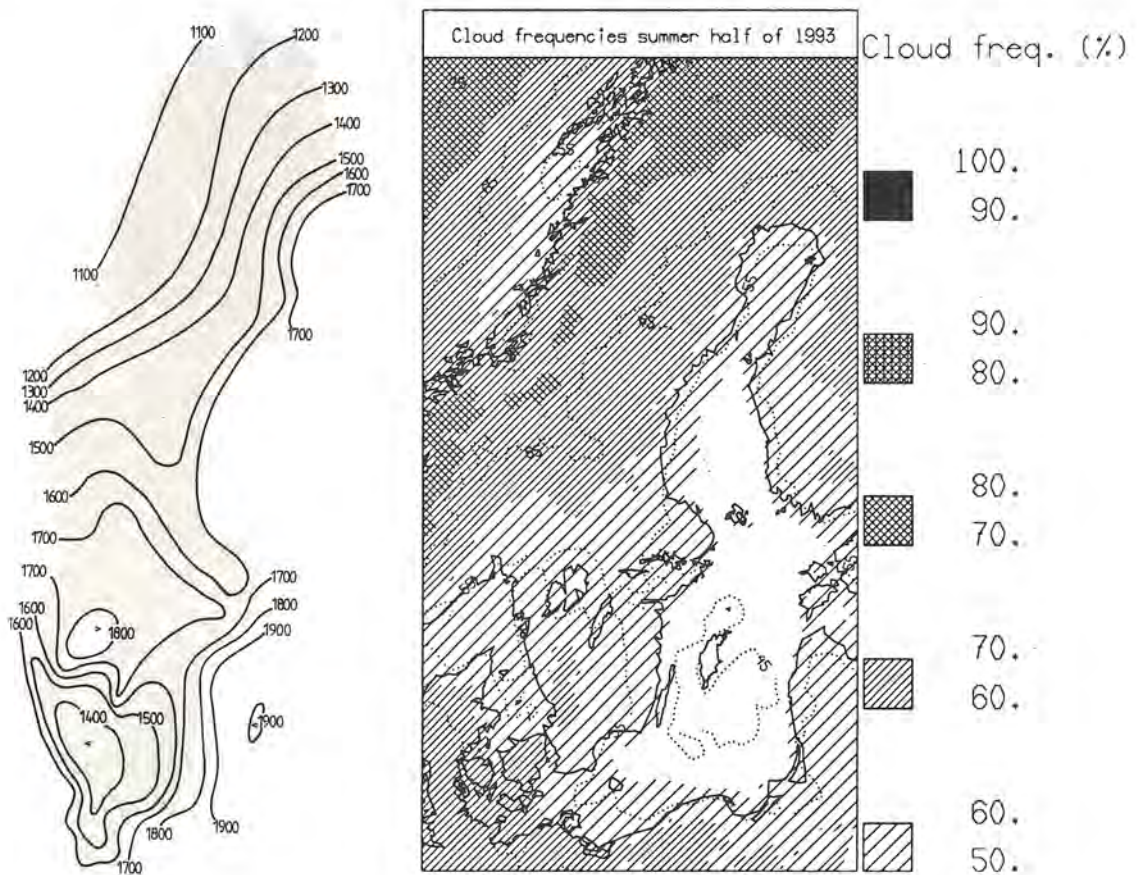


Figure 22. Accumulated sunshine duration (hours) in Sweden 1993 (left) and satellite-derived cloud frequencies April - September 1993 (right).

Another way to verify the satellite cloud information is to compare cloud frequencies with measured solar radiation from a network of observing stations in Sweden. Figure 22 (left part) shows an analysis of the accumulated sunshine duration in Sweden in 1993 (SMHI, 1994). This quantity should be highly correlated to cloud frequencies. The majority of the accumulated solar time generally occurs in the summer half of the year. When considering that the satellite analyses seem to be of excellent quality in the summer half of the year (as shown in Section 5.1), a comparison with measured sunshine duration seems most appropriate. A comparison can be made to the mean of cloud frequencies for the period April - September in the right part of Figure 22. Satellite data have here a horizontal resolution of 20 km. The satellite data reproduce the pattern of accumulated sunshine duration in most of its details. This supports and strengthens the conclusion that satellite analyses are of very high quality in summer.

### 5.3 Diurnal variation of cloud frequencies in June and in December

As usable satellite scenes are available four times each day, some information about the diurnal variation can be extracted. This section presents a comparison of derived cloud frequencies in June and in December 1993. The choice of these two months was done to study the differences between sunny and dark conditions. In June, we have a maximum in incoming solar radiation and also in the daily variation of received solar radiation at the surface. The opposite is true in December. Two interesting questions are: Do we still have a daily variation in cloud frequencies in December and are differences between land and sea areas found throughout the day in June?

Figure 23 shows cloud frequencies, with a horizontal resolution of 20 km, in June in early morning and morning (as defined in Table 6). The same is shown in Figure 24 for afternoon and evening conditions. We can clearly observe a pronounced daily variation in cloud frequencies over land surfaces. Here, the minimum in cloud frequencies is recorded in the early morning. A maximum is reached in the afternoon, generally between 60 - 80 % but at some places higher than 90%. The situation is very different for sea areas. A much smaller variation is seen here and in some places even reversed in time compared to land areas. Highest cloud frequencies are found in the early morning while the minimum seems to occur in the afternoon or in the evening. This situation leads to very sharp gradients in cloud frequencies at some places. Notice especially the situation in and around the Gulf of Bothnia in the afternoon (Figure 24, to the left). Here, a minimum of cloud frequencies below 30% is found at sea but inland, very close to the coast, cloud frequencies above 90% are common.

Figures 25 and 26 show the same kind of data for December. If we compare with the monthly mean (Figure 13 and Appendix), we conclude that the diurnal variation of cloud frequencies in December seems to be almost negligible. The found differences are small and may be caused partly by the low number of samples (approximately 27 - 30 for each time of day).

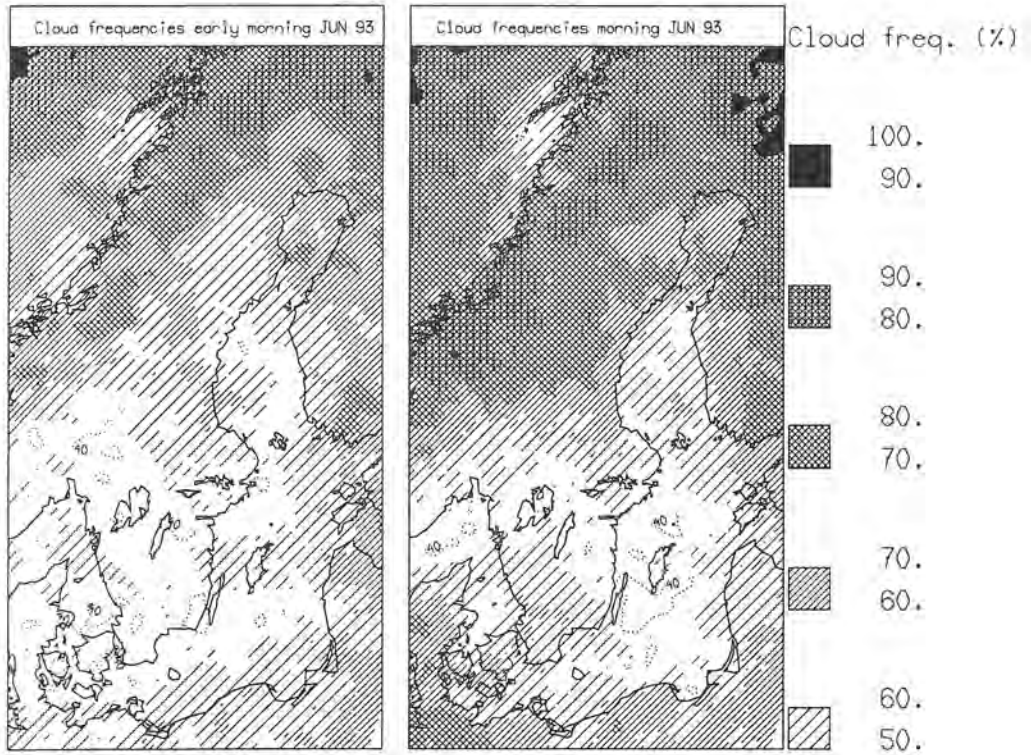


Figure 23. Satellite-derived cloud frequencies in the early morning (left) and in the morning (right) for June 1993.

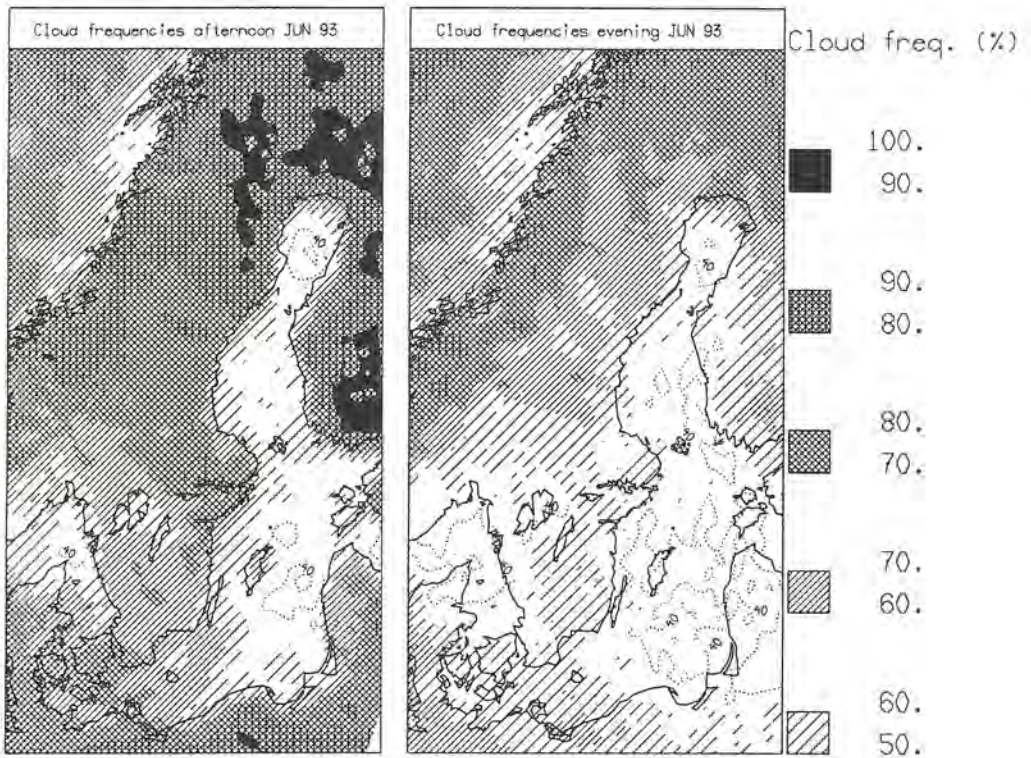


Figure 24. Satellite-derived cloud frequencies in the afternoon (left) and in the evening (right) in June 1993.

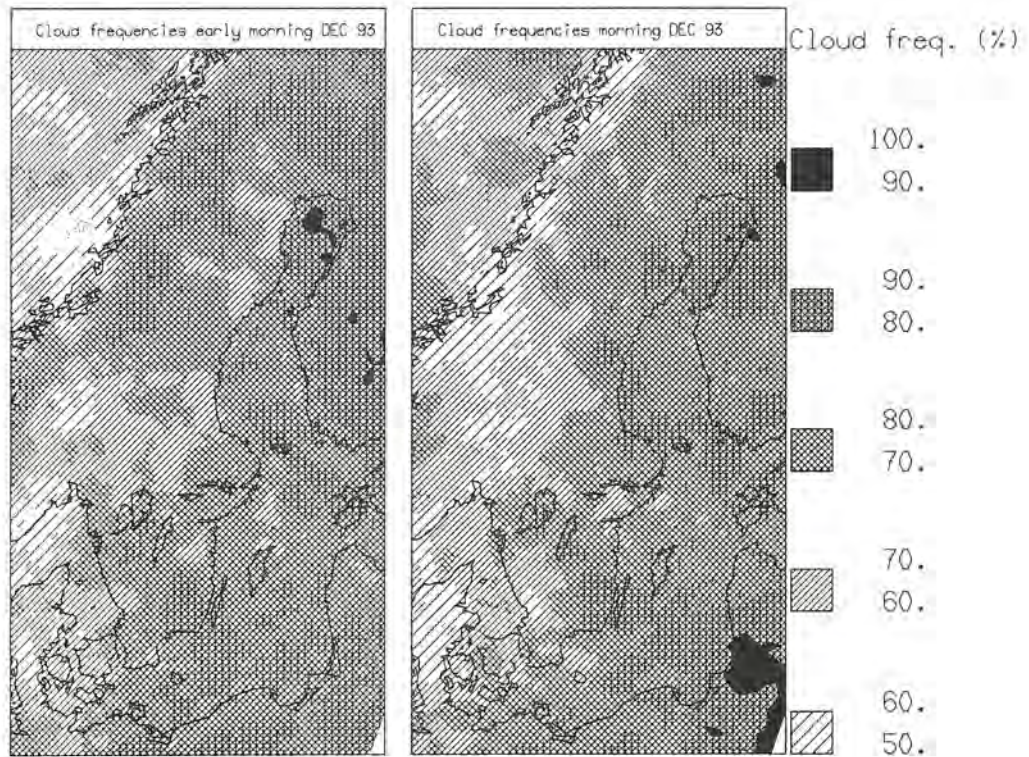


Figure 25. *Satellite-derived cloud frequencies in early morning (left) and in morning (right) in December 1993.*

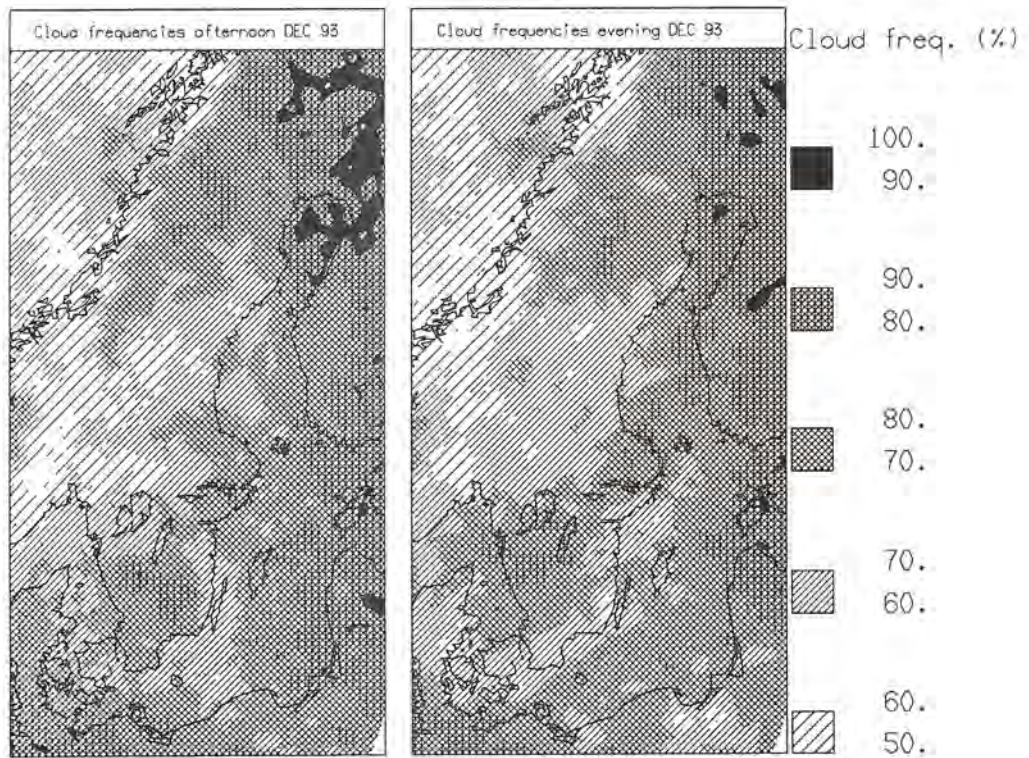


Figure 26. *Satellite-derived cloud frequencies in afternoon (left) and in evening (right) in December 1993.*

## 6. DISCUSSION

### 6.1 Cloud conditions monitored by SCANDIA

This report demonstrates that multispectral high resolution imagery from the NOAA AVHRR instrument can be used to describe mean cloud conditions in the Nordic area for an entire year. The mean fractional cloud cover in 1993, represented as cloud frequencies for individual pixels, is analysed by using cloud classifications provided by the SCANDIA model. Comparisons with surface observations show very satisfying results, both in the description of local scale details and in the general description of synoptic scale conditions.

Differences in surface characteristics are shown to modify cloud conditions strongly. Even though this is a well-known fact, the presented method offers a mean to quantify the difference, which is difficult when using only conventional surface observations. The difference between land and sea areas is especially pronounced during the summer half of 1993. Much lower cloud frequencies are found over sea areas than over land. This is seen in both cloudy cyclonic weather types and in less cloudy anticyclonic weather types. The suppression of cloud formation over sea areas in the summer half of 1993 is strong enough to be seen also in the annual mean, at least for major parts of sea areas.

The absolute minimum in cloud frequencies in 1993 is found in the Baltic Sea between the Swedish mainland and the island of Gotland. It is interesting to notice that two of the nearby SYNOP stations here, Ölands Norra Udde and Stora Karlsö, sometimes have been suspected to report too low precipitation amounts. The cloudiness minimum indicates that the reported precipitation amounts may be correct. However, it is not clear whether the minimum in cloudiness here is a typical feature that also can be seen in a longer time perspective.

Orographic effects are also indicated, leading to increased cloudiness in mountainous areas as well as to decreased cloudiness downwind in the lee of mountain ranges. The dependence on altitude is noticeable even for low elevations (e.g. for the inner and western part of southern Sweden with elevations of only 300 - 400 m). Naturally, the lee effects, indicated in the winter half of the year, appear in connection with long periods of strong westerly winds.

Cloud conditions over the Norwegian Sea are found to be particularly interesting. A well-defined minimum in cloud frequencies is identified close to the Norwegian coast. The minimum is seen for individual months as well as in the annual mean. We suggest that the minimum is caused by a combination of thermal and orographic forcing. A weak minimum in sea surface temperatures is found in spring and in early summer close to the Norwegian coast, maybe as a result of the melting snow in the mountains. Such a minimum should weaken the convective activity here. Areas further offshore have somewhat higher temperatures due to the influence from the main core of the Gulf stream. Thus, convective clouds then form more easily here. Inland, the Norwegian mountains generate both convective and orographic clouds throughout the year. These circumstances interact creating conditions for a minimum in cloud frequencies to form

near the coast. The possibility of a lee effect, caused by dominating easterly winds, is not supported by mean circulation patterns.

## 6.2 Quality of SCANDIA results

SCANDIA results are found to be of very high quality during the spring, summer and autumn seasons. A separate study (Karlsson, 1994) presents and discusses specifically monthly cloud frequencies in May, June, July and August 1993. Comparisons with surface observations in summer suggest that the surface observer overestimates cloud amounts systematically, especially in cases with convective cloud types. The overestimation appears to be of the order of 1 - 2 octas with the highest overestimation for reported cloud amounts between 5 and 8 octas.

The most serious limitation of the SCANDIA model is the small but noticeable underestimation of cloud frequencies in dark conditions (at night and near sunrise/sunset), especially in the winter season. Apparently, the separability of cloud-free areas, from either low level water droplet clouds at very low sun elevations (2 - 6°) or from thin Cirrus clouds superimposed over low level water droplet clouds at night, is poor when using image data alone. The situation may be improved if auxiliary data (*a priori* surface temperatures, e.g. extracted from short-range weather forecasts) are utilized. However, the improvement is possible only in the absence of strong low-level temperature inversions. If such inversions are present, the non-separability of cloud-free areas from cloudy areas persists. A new version of the cloud classification method, using short forecasts of surface temperatures from the HIRLAM model, has recently been introduced operationally, and preliminary results are promising. Careful tuning is, however, necessary to minimize the sensitivity of inherent errors in surface temperature forecasts.

## 6.3 Resemblance to true cloud frequencies

It may be questioned how close is the satellite-estimated cloud frequency to the true mean cloudiness for an individual day or a month? Only four observations per day may seem insufficient here. Studies of the results, having a maximum horizontal resolution of 4 km, show that the small scale variation from pixel to pixel is often large. The magnitude of the small-scale variation is sometimes too high to be found realistic and this suggests that undersampling may be at hand and/or that the way to compute cloud frequencies is inadequate. One may suggest that mean values computed for larger areas (e.g. with 20 km resolution as presented in the Appendix) should be more representative for mean cloud conditions. The use of only four observations per day is not an obvious limitation on this coarser scale. Although the formation and decay of individual cloud elements may be rapid, larger scale cloud patterns (e.g. Cumulus cloud ensembles and streets, Stratus cloud areas and Nimbostratus cloud systems) change and move rather slowly. Mean cloud conditions would then be possible to estimate from high resolution satellite imagery, at least if results are averaged on a coarser resolution.

#### 6.4 Sensitivity to AVHRR sensor noise and degradation

The study shows that SCANDIA results can be used both as a real-time diagnostic tool in weather forecasting and for monitoring long-term cloud conditions (total fractional cloud cover) in climate analysis. Total fractional cloud cover is, however, only one of many crucial cloud parameters of importance when investigating the role of clouds for climate. Other important parameters are cloud albedos, cloud water content, cloud droplet spectra and cloud water phase. Some of them are also possible to estimate from satellite measurements (e.g. Arking and Childs (1985) and Kriebel *et al.* (1989)).

Cloud classifications from SCANDIA are indirectly based on the above-mentioned parameters as they affect all the derived features for the classification model (Table 2). The quality of estimations of these parameters is highly depending on the accuracy of available calibration methods, especially since no onboard calibration of visible radiometer channels normally exists. Currently used calibration methods applied on AVHRR visible channels have been subject to changes (Teillet, 1992) and are still carefully investigated. Furthermore, along-time degradation of AVHRR visible measurements has been observed (Brest and Rossow, 1992). It means that also time-dependent corrections of visible radiometer measurements are necessary if long-term use of AVHRR data from different satellites is intended (Che and Price, 1992). These problems in establishing an absolute calibration of AVHRR visible channels have so far made an efficient use of AVHRR data for climate studies partly difficult.

The noticed degradation with time of visible AVHRR measurements has not yet been found to affect cloud analyses from SCANDIA severely. The explanation is probably that SCANDIA relies more on the infrared channels (especially AVHRR channel 3) than on the visible channels. On the other hand, it means that SCANDIA is sensitive to noise problems in the infrared channels (Dudhia, 1989). Specific problems have been found for AVHRR channel three. The noise is most seriously affecting SCANDIA results when studying very cold objects. It causes an overestimation of cloud cover in very cold, cloud-free areas and thus partly explains the somewhat lower quality of cloud observations from SCANDIA in winter. Reduction of noise levels in channel three for future AVHRR instruments should improve results from SCANDIA cloud analyses.

#### 6.5 Climate studies related to cloud forcing from Cirrus clouds and low-level clouds

We conclude here that an efficient use of all AVHRR channels does allow creation of realistic long-term analyses of cloud distributions at high latitudes. A description of the vertical distribution of clouds is also possible, since SCANDIA produces a separation into different cloud types. The quality of such information has still to be investigated. A study investigating the skill of the cloud type separation is now initiated, using the same verification data set as earlier discussed in Section 4. Some problems have already been indicated when separating small-scale Cumulus clouds from thin Cirrus clouds. Such an error is serious if results are intended for use in climate studies. This is evident when considering the cooling effect on the atmosphere-earth system, caused by low-level water clouds in the solar short-wave spectrum, compared to the warming effect in the

terrestrial long-wave spectrum, caused by thin Cirrus clouds (see Ramanathan *et al.* (1989) and Arking (1991)). Improving the separation of Cirrus and Cumulus clouds will be focused in future revisions of the SCANDIA model.

A technical problem of climatological importance, beside the earlier discussed sensor problems, is the instability of the sun-synchronous orbits of the different NOAA-satellites. Equator-crossing times for the satellites NOAA-9 and NOAA-11 have been shown to deviate towards later passage times after some years. A long-term study of the seasonal and annual variation of cloud conditions for climatological purposes is then made difficult, since observation times are changing.

Another technical problem in the future will be the coming changes of the spectral bands of the AVHRR instrument introduced on NOAA-K (NOAA-15). A new spectral band at 1.6  $\mu\text{m}$  will be used during daytime, replacing the present AVHRR channel 3. The switch between the two bands day and night imposes a redefinition of the SCANDIA model and introduces a complicated model structure. It is not obvious that the new spectral band will improve classification results, since we are at present very satisfied with the daytime performance of the 3.7  $\mu\text{m}$  channel.

## 6.6 Future use and improvement of SCANDIA cloud analyses

Cloud analyses from SCANDIA are continuously archived since February 1991, and they are available with a selection of verifying surface observations. Diagnosis of annual and monthly cloud frequencies is then feasible also for 1991 and 1992. Continued archiving and improved methods should enable future analyses of cloudiness for periods containing several years.

Improved compensations for varying sun elevations and regional airmass differences have recently been implemented in a new SCANDIA version. Cloud analyses on larger regional scales (e.g. northwestern Europe) are now made possible. Improved corrections for high satellite zenith angles and enhanced anisotropic reflection will also be developed in the near future. Such corrections may increase the number of usable satellite scenes from four to 8 - 12 per day for the Nordic area, thus allowing a more accurate description of daily cloud conditions.

SCANDIA cloud information is also considered for use within the concept of a mesoscale objective analysis scheme, together with other sources of cloud observations. Such a scheme is now developed using the HIRLAM forecasting system with a horizontal resolution of 20 km. A quality control scheme for the SCANDIA cloud information will then be constructed to remove data when the separability of clouds from other surfaces is low in AVHRR imagery. *A priori* information of sun elevations, satellite elevations and temperature conditions in the satellite scene will be used for that purpose. The mesoscale analysis will eventually be able to produce more accurate analyses of daily and seasonal cloudiness by reducing the undersampling of cloud observations being present when using satellite observations alone. Experiments will furthermore be carried out using METEOSAT imagery to increase the number of available satellite observations in the mesoscale analysis process.

Beside the mesoscale analysis product, automatically produced high-resolution (down to 1 km) cloud analyses from NOAA AVHRR data alone should also be feasible by utilizing the envisaged system for quality control.

## **6.7 Proposals of future studies**

Interesting future studies could be devoted to comparing estimated cloud cover statistics from SCANDIA with modelled cloudiness from atmospheric circulation models. Comparisons can be applied to both ordinary numerical weather prediction models as well as to general circulation models used in climate research.

Another interesting topic could be to compare SCANDIA cloud analyses with global cloud analyses from the ISCCP (International Satellite Cloud Climatology Project - see Schiffer and Rossow, 1983) algorithms for Polar areas and for areas at high latitudes. The present ISCCP algorithms have been found inadequate here (Mokhov and Schlesinger, 1993). The concept of using multispectral information from the full five-channel AVHRR data set should therefore be considered. The use of AVHRR imagery with maximum horizontal resolution is furthermore proposed since a resampling of image data to a coarser resolution may destroy the separability of certain cloud types. Especially the use of AVHRR channel 3 is critical in this respect. Night-time signatures of thin Cirrus clouds and low-level water clouds are opposite but very different to cloud-free areas when comparing brightness temperatures in AVHRR channels 3 and 4. An averaging of radiances to a coarser resolution may cancel these spectral differences. A separation of Cirrus clouds and low-level water clouds is then made more difficult. The situation is even worse if the land surface temperature is comparable with existing cloud temperatures, a situation that is very common in high latitudes and in the Polar areas. A mixing of radiances from Cirrus clouds and low-level water clouds may then result in the erroneous classification into a cloudfree pixel. The basic cloud discrimination should therefore be performed at maximum horizontal resolution to minimize the error caused by mixing of spectral signatures. The final cloud analysis may later be averaged to a coarser resolution, if that is preferred.

A third area of interest would be to investigate the possibility to model the input of solar radiation at the surface by using the satellite-retrieved cloud information. SCANDIA results are able to reproduce the main pattern of recorded sunshine duration in Sweden in 1993. This indicates that there is a potential to compute also the accumulated amount of solar radiation from the satellite information.

Finally, a fourth area of interest would be to investigate the correlation of the retrieved cloud information to monitored algal bloom episodes in the Baltic Sea and other sea areas (Håkansson and Moberg, 1993). Such episodes are related to long periods of high solar radiation at the sea surface without clouds. The correlation to mean cloud conditions and the dependence of other important factors have still to be investigated.

## ACKNOWLEDGEMENTS

The author is greatly indebted to Erik Liljas at SMHI for assisting when constructing the SCANDIA model. His knowledge of multispectral signatures in weather satellite imagery has been truly invaluable. Valuable comments on the manuscript have been given by Hans Alexandersson and Erik Liljas. The author also thanks Eva Zacke and Eva Lena Ljungkvist for assisting with some of the figures.

## REFERENCES

- Arking, A. 1991.  
The radiative effects of clouds and their impact on climate.  
Bull. Am. Meteor. Soc. Vol. 71 No. 6, p. 795-813.
- Arking, A. and Childs, J. D. 1985.  
Retrieval of cloud cover parameters from multispectral satellite measurements.  
J. Clim. Appl. Meteor. 24, p. 322-333.
- Bordes, P., Brunel, P. and Marsouin, A. 1992.  
Automatic adjustment of AVHRR navigation.  
J. Atm. Ocean. Techn. Vol. 9 No. 1, p. 15-27.
- Brest, C. L. and Rossow, W. B. 1992.  
Radiometric calibration and monitoring of NOAA AVHRR data for ISCCP.  
Int. J. Rem. Sens. Vol. 13 No. 2, p. 235-273.
- Che, N. and Price, J. C. 1992.  
Survey of Radiometric Calibration Results and Methods for Visible and Near Infrared Channels of NOAA-7, -9 and -11 AVHRRs.  
Rem. Sens. Env. 41, p. 19-27.
- Coakley, J. A. and Bretherton, F. P. 1982.  
Cloud cover from high resolution scanner data: detecting and allowing for partially filled fields of view.  
J. Geophys. Res. 87, C7, p. 4917-4932.
- Derrien, M., Farki, B., Harang, L., LeGléau, H., Noyalet, A., Pochic, D. and Sairouni, A., 1993.  
Automatic cloud detection applied to NOAA-11/AVHRR imagery.  
Rem. Sens. of Env., 46, p. 246-267.
- Dudhia, A. 1989.  
Noise characteristics of the AVHRR infrared channels.  
Int. J. Rem. Sens. Vol. 10 Nos. 4 and 5, p. 637-644.

- d'Entremont, R. P. 1986.  
Low- and midlevel cloud analysis using nighttime multispectral imagery.  
J. Climate Appl. Meteor. Vol. 25 No. 12, p. 1853-1869.
- Eyre, J. R., Brownscombe, J. L. and Allam, R. J. 1984.  
Detection of fog at night using Advanced Very High Resolution Radiometer (AVHRR) imagery.  
Meteor. Mag. 113, p. 266-271.
- Gustafsson, N., 1991.  
The HIRLAM model.  
Proceedings of Seminar on Numerical Methods in Atmospheric Models. ECMWF, Reading, UK, 9-13 September 1991.
- Hoyt, D. V. 1977.  
Percent of possible sunshine and total cloud cover.  
Mon. Wea. Rev. 105, p. 648-652.
- Håkansson, B. G. and Moberg, M. 1993.  
The algal bloom in the Baltic during July and August 1991, as observed from the NOAA weather satellites.  
Accepted for publication in Int. J. Rem. Sens.
- Inoue, T. 1987.  
Cloud type classification with NOAA-7 split window measurements.  
J. Geophys. Res. 4, p. 3991-4000.
- Karlsson, K-G. 1989.  
Development of an operational cloud classification model.  
Int. J. Remote. Sens., Vol. 10, Nos 4-5. p. 687-693.
- Karlsson, K-G. 1993.  
Comparison of operational AVHRR-based cloud analyses with surface observations.  
In Proc. 6th European AVHRR Data Users' Meeting, Belgirate, Italy, 28 June - 3 July, 1993, EUMETSAT, p. 223-230.
- Karlsson, K-G. 1994.  
Cloudiness in the Nordic summer season estimated from multispectral satellite measurements.  
Accepted for publication in AMBIO.
- Karlsson, K-G. and Liljas, E. 1990.  
The SMHI model for cloud and precipitation analysis from multispectral AVHRR data.  
PROMIS Report 10, SMHI.
- Kidder, S. Q. and Wu, H. 1984.  
Dramatic contrast between low clouds and snow cover in daytime 3.7  $\mu\text{m}$  imagery.  
Mon. Wea. Rev. Vol. 112 No. 11, p. 2345-2346.

- Kriebel, K. T., Saunders, R. W. and Gesell, G. 1989.  
Optical properties of clouds derived from fully cloudy pixels.  
Beitr. Phys. Atmosph. 62, p. 165-171.
- Lauritson, L., Nelson, G. J. and Porto, F. W. 1979.  
Data extraction and calibration of TIROS-N/NOAA radiometers.  
NOAA Technical Memo NESS 107, NOAA, Washington D. C.
- Liljas, E. 1981.  
Analysis of clouds and precipitation through automated classification of AVHRR data.  
SMHI Reports, RMK 32.
- Mokhov, I. I. and Schlesinger, M. E. 1993.  
Analysis of global cloudiness. 1. Comparison of Meteor, Nimbus 7 and International  
Satellite Cloud Climatology Project (ISCCP) Satellite data.  
J. Geoph. Res., Vol. 98, No. D7, p. 12 849 - 12 868.
- Phulphin, T., Derrien, M. and Brard, A. 1983.  
A two-dimensional histogram procedure to analyse cloud cover from NOAA satellite  
high resolution imagery,  
J. Climate. Appl. Meteor. Vol. 22 No. 8, p. 1332-1345.
- Ramanathan, V., Barkstrom, B. R. and Harrison, E. F. 1989.  
Climate and the earth' s radiation budget.  
Physics today, May 1989, p. 22-32.
- Saunders, R. A. and Gray, D. E. 1985.  
Interesting cloud features seen by NOAA-6 3.7  $\mu\text{m}$  images.  
Meteor. Mag. Vol. 114 No. 1356, p. 211-214.
- Saunders, R. W. and Kriebel, K. T. 1988.  
An improved method for detecting clear sky and cloudy radiances from AVHRR data.  
Int. J. Remote Sens., Vol. 9, No 1, p. 123-150.
- Schiffer, R. A. and Rossow, W. B. 1983.  
The International Satellite Cloud Climatology Project (ISCCP). The first project of the  
World Climate Research Programme.  
Bull. Am. Meteor. Soc. Vol. 64 No. 7, p. 779-784.
- SMHI, 1993-1994.  
Väder och Vatten: January 1993 - January 1994. Monthly weather and climate  
summaries (in Swedish).
- SMHI, 1994.  
Väder och Vatten: Väderåret 1993. Summary of weather and climate for the year of  
1993 (in Swedish).

Teillet, P. M. 1992.

An algorithm for the radiometric and atmospheric correction of AVHRR data in the solar reflective channels.

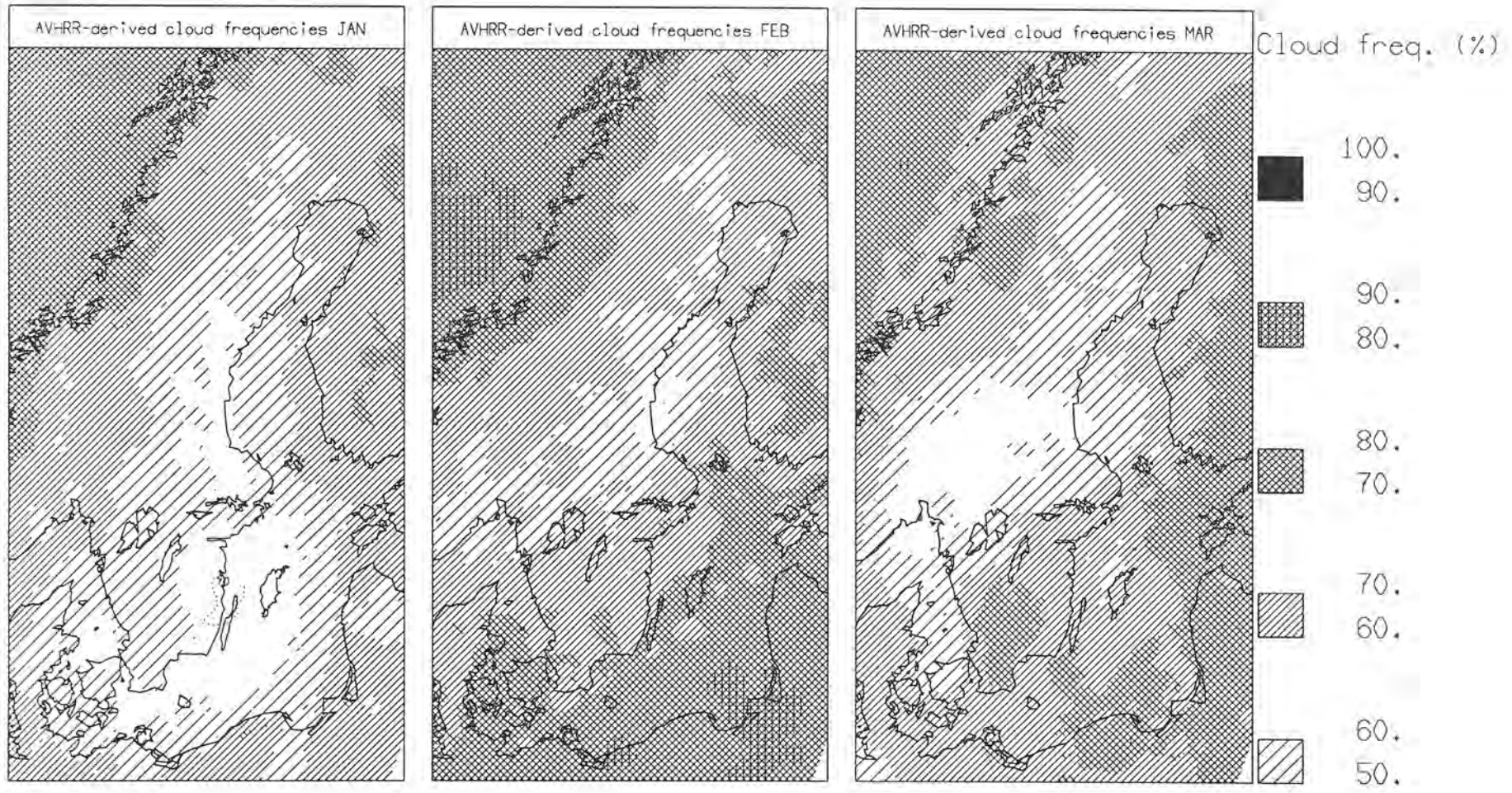
Rem. Sens. Env. Vol. 41 Nos. 2 and 3, p. 185-195.

## APPENDIX

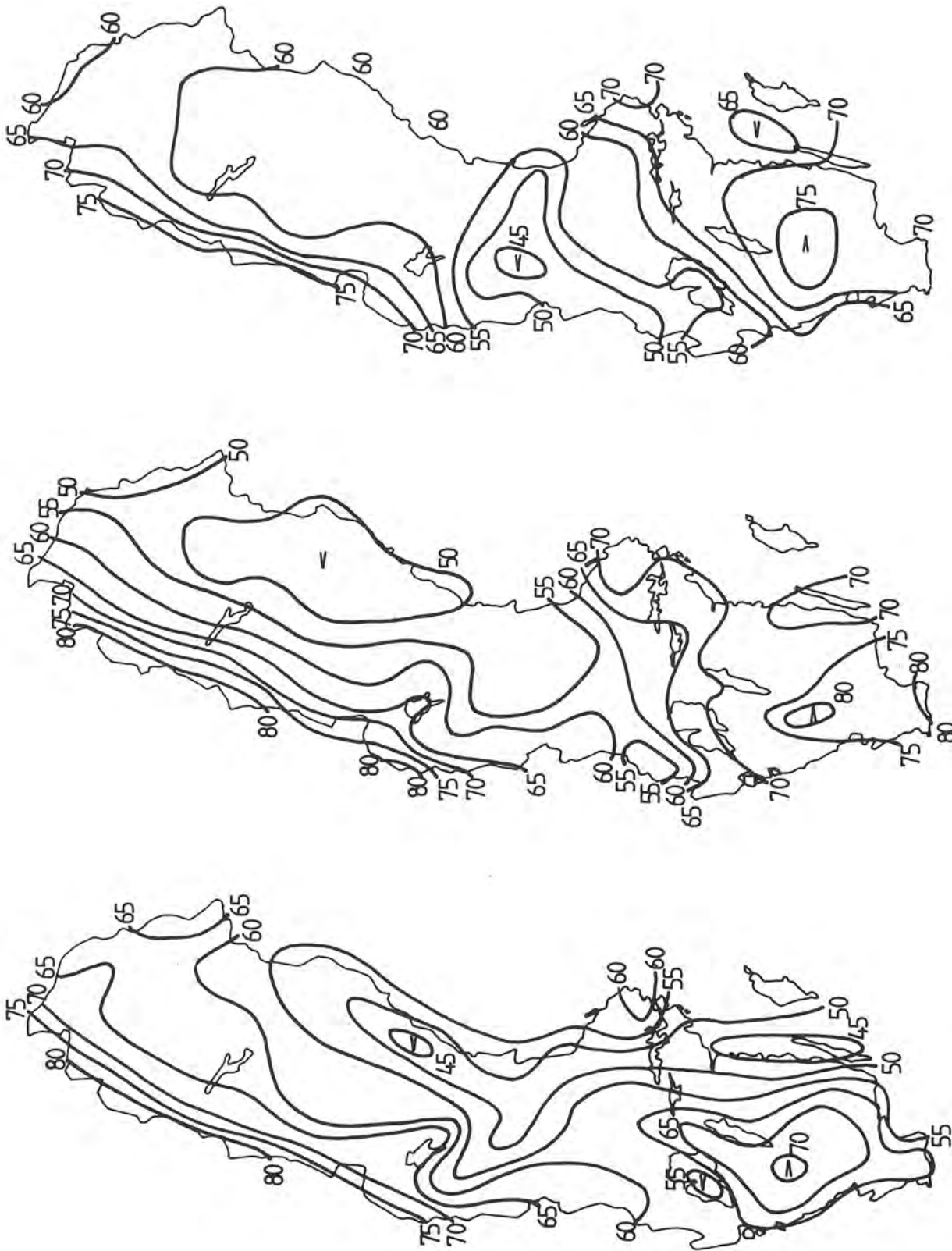
The following pages show comparisons of SYNOP computed mean cloudiness and satellite-retrieved cloud frequencies for all months of 1993.

SYNOP analyses of mean cloudiness (in %) are based on cloud observations 06, 12 and 18 UTC. Isolines in intervals of 5% were drawn subjectively.

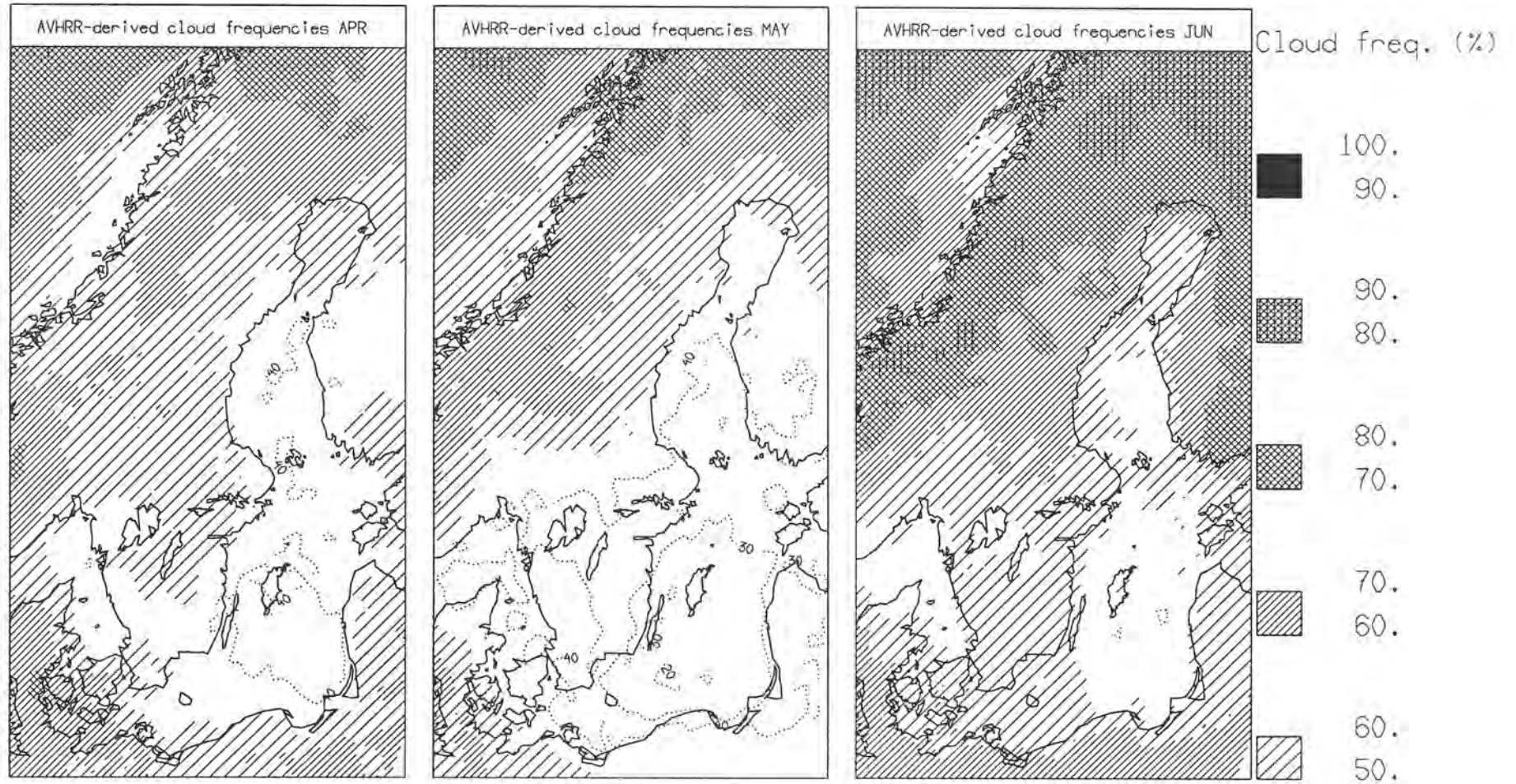
Satellite-derived analyses are based on the data shown in Figures <sup>15-18</sup>10-13. Averages have been computed with a horizontal resolution of 20 km. Results are shown in intervals of 10% with isolines between 0-50% and with various levels of hatchings between 50 - 100%.



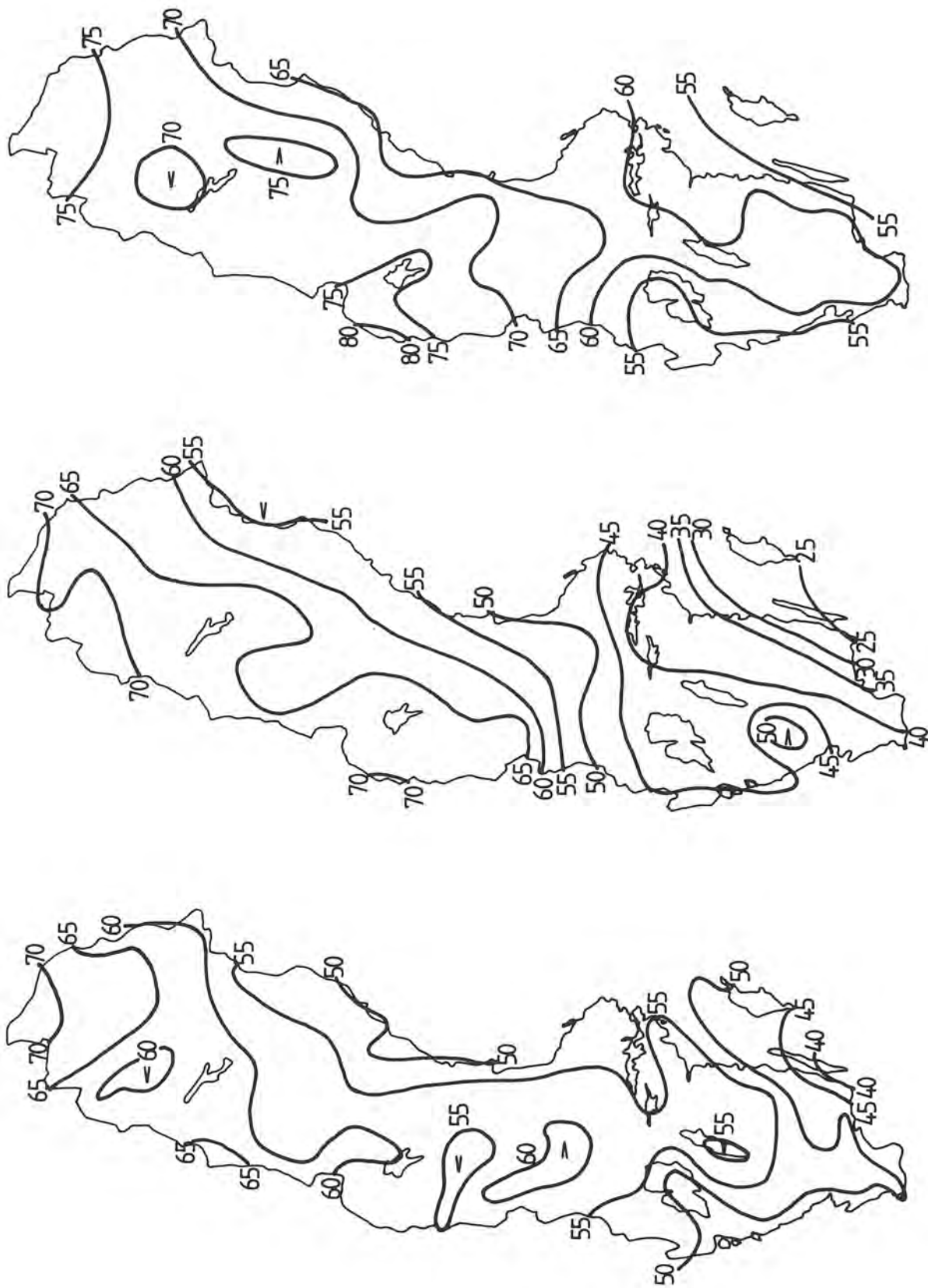
Monthly cloud frequencies in 1993 from AVHRR for the months of January (left), February (centre) and March (right).



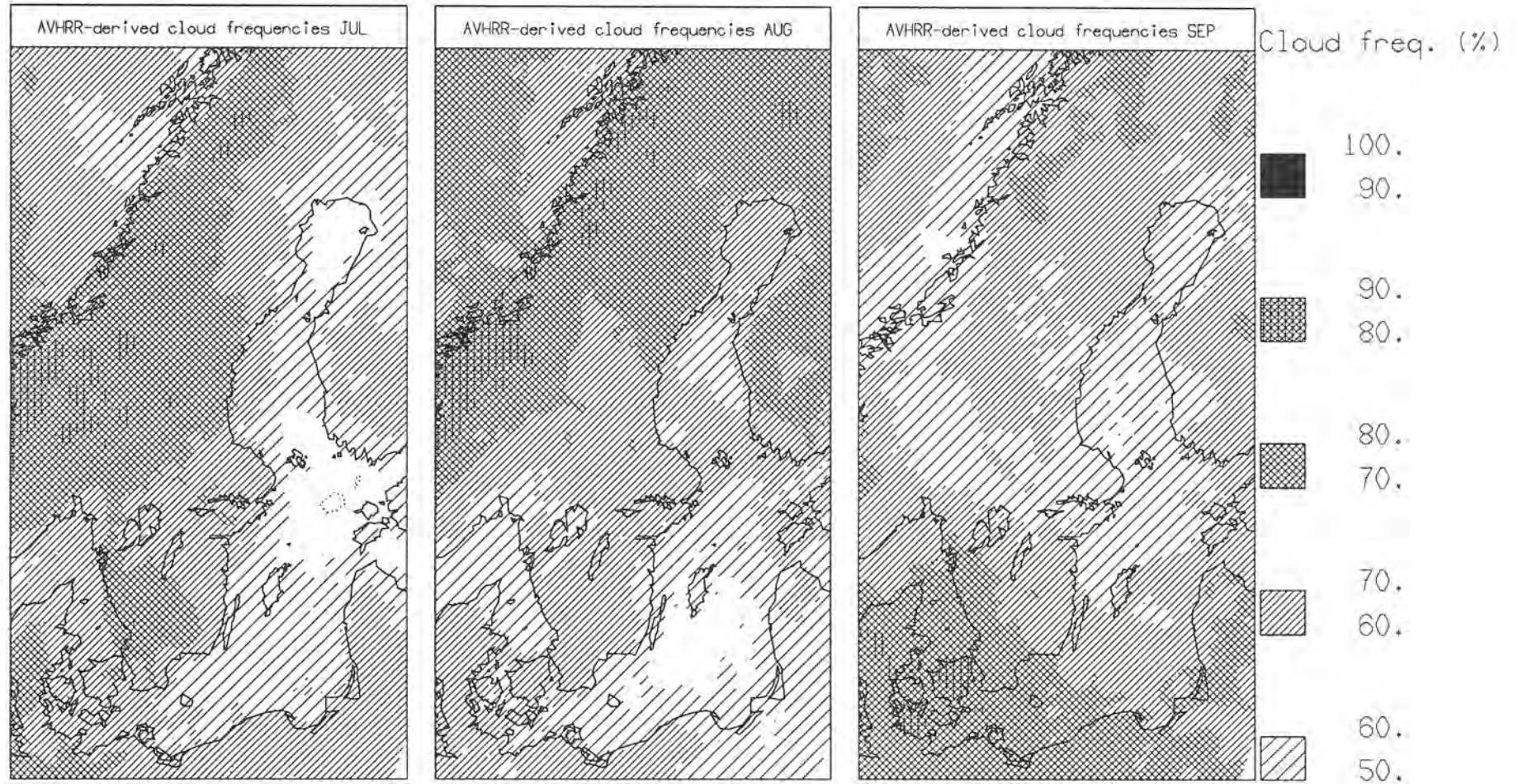
Mean cloudiness (%) from SYNOP in 1993 for the months of January (left), February (centre) and March (right).



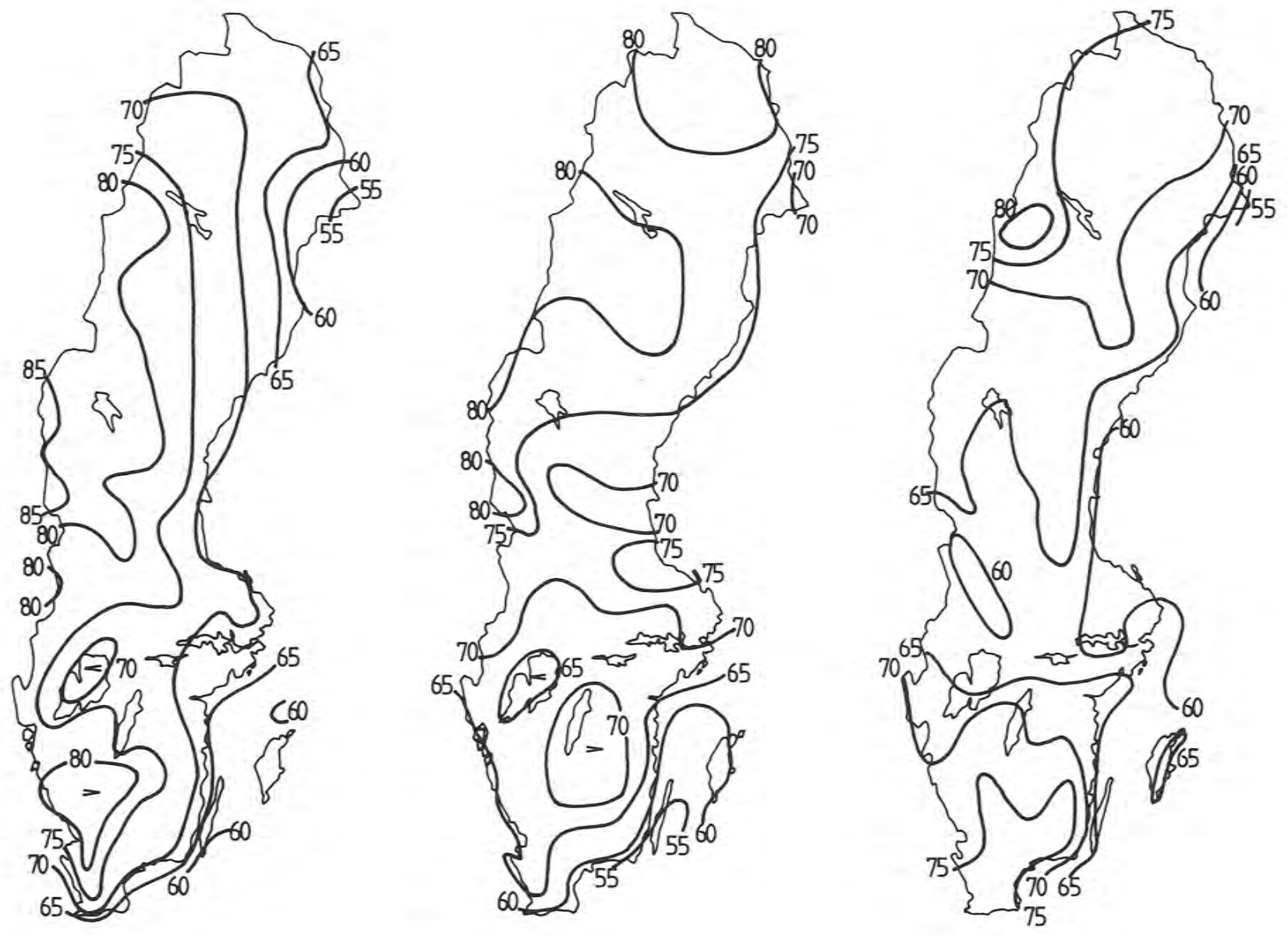
Monthly cloud frequencies in 1993 from AVHRR for the months of April (left), May (centre) and June (right).



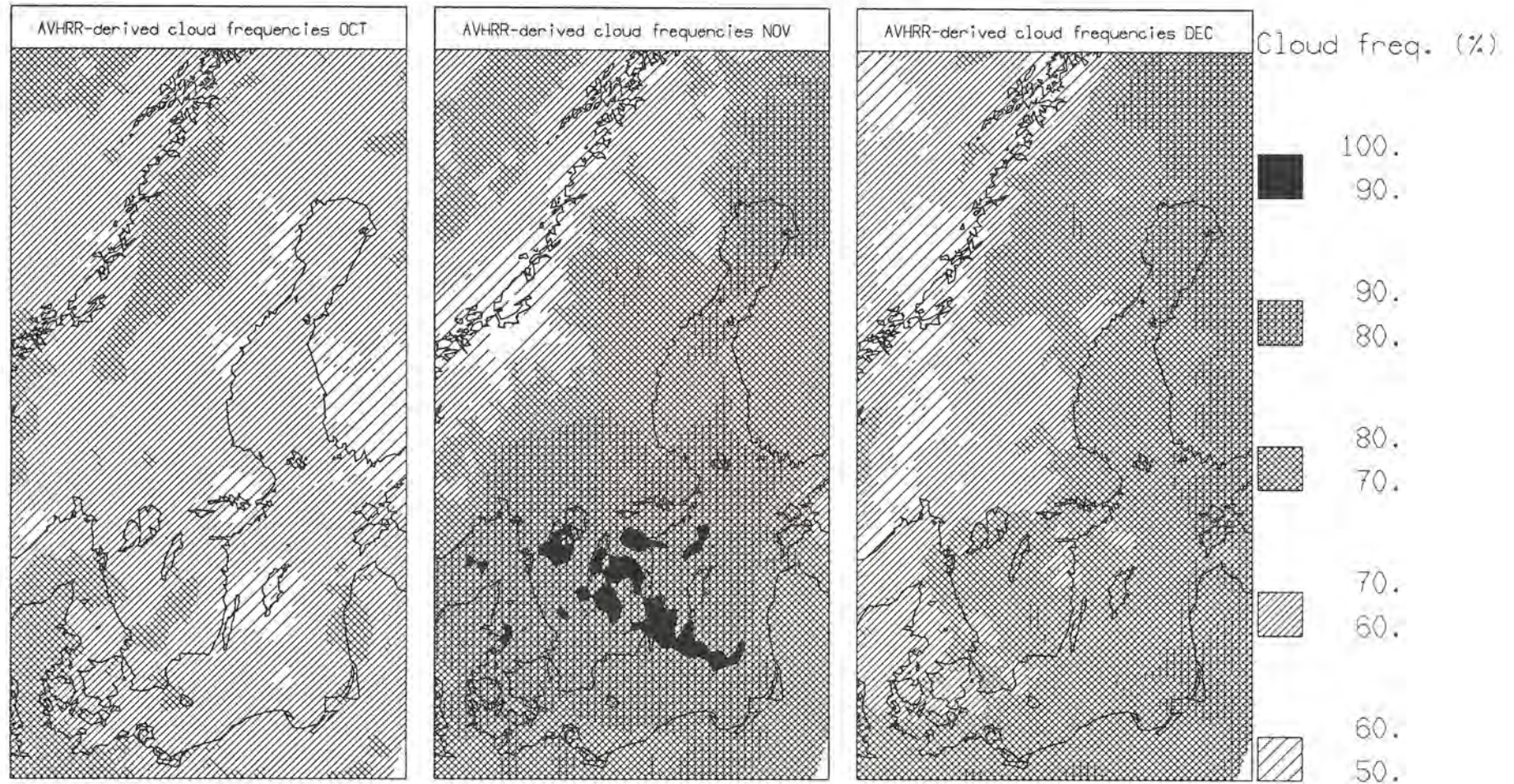
Mean cloudiness (%) in 1993 from SYNOP for the months of April (left), May (centre) and June (right).



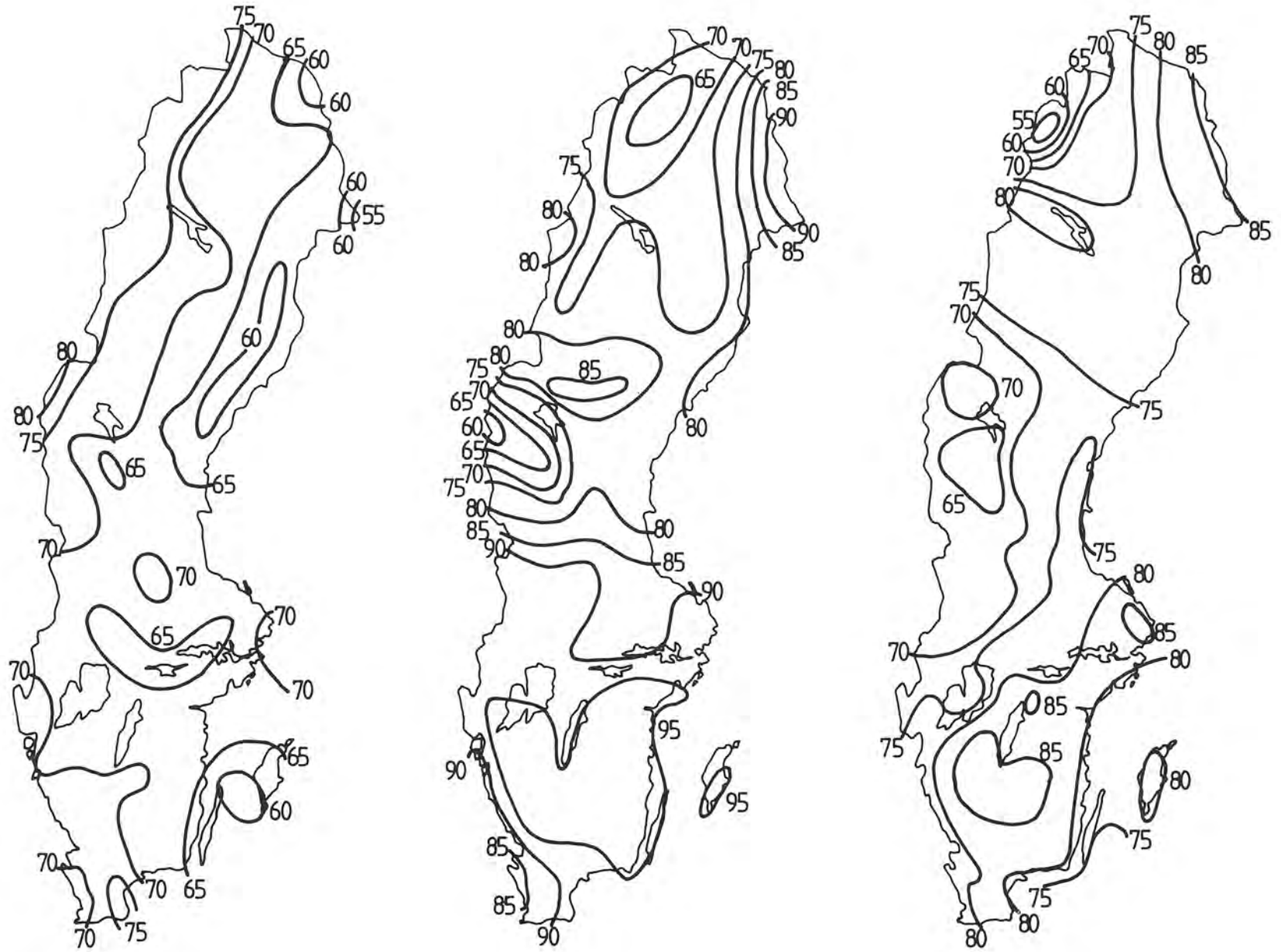
Monthly cloud frequencies in 1993 from AVHRR for the months of July (left), August (centre) and September (right).



Mean cloudiness (%) in 1993 from SYNOP for the months of July (left), August (centre) and September (right).



*Monthly cloud frequencies in 1993 from AVHRR for the months of October (left), November (centre) and December (right).*



Mean cloudiness (%) in 1993 from SYNOP for the months of October (left), November (centre) and December (right).











Swedish meteorological and hydrological institute  
S-601 76 Norrköping, Sweden. Tel. +4611158000. Telex 644 00 smhi s.